



Residual Stresses in Hollow Section Joint

**Czech Technical University in Prague
Faculty of Civil Engineering
Department of steel and timber structures
Erasmus Mundus: SUSCOS 2016-18**



Author: Kovil Chaitanya Reddy R A

Supervisor: prof. Ing. František Wald, CSc.



**Czech Technical University in Prague
Department of Steel and Timber Structures**



ČESKÉ VYSOKÉ UČENÍ TECHNICKÉ V PRAZE

Fakulta stavební
Thákurova 7, 166 29 Praha 6

ZADÁNÍ DIPLOMOVÉ PRÁCE

I. OSOBNÍ A STUDIJNÍ ÚDAJE

Příjmení: RODDAM APPIREDDY Jméno: Kovil Chaitanya Reddy Osobní číslo: 469114
Zadávající katedra: 1134
Studijní program: SUSCOS
Studijní obor: Civil Engineering

II. ÚDAJE K DIPLOMOVÉ PRÁCI

Název diplomové práce: _____

Název diplomové práce anglicky: Residual stresses in hollow section joints

Pokyny pro vypracování:

State of the Art
FEA advanced model
FEA design mode
Sensitivity study
Summary


Seznam doporučené literatury:


T.R. Gurney, Fatigue of Welded Structures, Cambridge Univ. Press (1979)
J. Krebs, M. Kassner, Alstom-LHB (2007), "Influence of welding residual stresses on fatigue design of welded joints and components", Welding in the World, Vol. 51, n° 7/8.
J. Wardenier, "Hollow sections in structural applications", Comité International pour le Développement et l'Etude de la Construction Tubulaire.

Jméno vedoucího diplomové práce: prof. František Wald

Datum zadání diplomové práce: 1 Oct 2017 Termín odevzdání diplomové práce: 7 Jan 2018

Údaj uveďte v souladu s datem v časovém plánu příslušného ak. roku


Podpis vedoucího práce



Podpis vedoucího katedry

III. PŘEVZETÍ ZADÁNÍ

Beru na vědomí, že jsem povinen vypracovat diplomovou práci samostatně, bez cizí pomoci, s výjimkou poskytnutých konzultací. Seznam použité literatury, jiných pramenů a jmen konzultantů je nutné uvést v diplomové práci a při citování postupovat v souladu s metodickou příručkou ČVUT „Jak psát vysokoškolské závěrečné práce“ a metodickým pokynem ČVUT „O dodržování etických principů při přípravě vysokoškolských závěrečných prací“.

1 Oct 2017

Datum převzetí zadání



Podpis studenta(ky)

Declaration

I hereby declare that this assignment is my own work and is not copied from any other person's work (published or unpublished), and has not previously submitted for assessment either at Czech Technical University in Prague or elsewhere and I have stated all information resources used in conformity with the Methodical guide for ethical development of university final thesis.

Prague, 7 January 2018

R A Kovil Chaitanya Reddy

Acknowledgements

I would like to express my sincere gratitude to my supervisor František Wald for his excellent guidance throughout this period. I couldn't have finished this thesis without his constant support and motivation. His valuable inputs, contributions, patience and encouragement have helped me complete my work and I am highly indebted to him.

I thank the Board of directors of the SUSCOS consortium for giving me this wonderful opportunity to pursue this degree and all my teachers for the knowledge they have shared during my time in SUSCOS.

I would like to thank Svitlana Kalmykova for providing the mechanical test results which were used for validation of the model used in this thesis.

In special, I would like to thank the Michal Jandera for contributing to this thesis with his great knowledge and time by the several discussions about the subject. I am grateful to him for his support and time.

I am grateful to my colleagues and friends for having faith in me and encouraging me to pursue my dreams. This journey would not have been the same without them.

Lastly, I would like to dedicate this thesis to my father, mother and brother, who have showered me with their unconditional love, support and encouragement. They are the reason for who I am today, and I look forward to fulfilling their wishes to the best of my ability.

Abstract

This dissertation presents a study involving the influence of Residual stresses on a hollow section T-Joint subjected to compressive axial load on the brace.

Nowadays, it is only possible to perform analytical solutions regarding this joint resistance capacity based on empirical formulas which are included on EC 1993-1-8.

The present study explores the development of numerical and analytical models to further understand the behavior of T-joint under residual stresses. The numerical model is built on FE software ABAQUS and is validated and verified with the experimental data. Residual stresses are applied in the Numerical model using solid and shell elements as presented in this thesis.

A Sensitivity study was carried out and included in this study to evaluate the influence of residual stresses on the resistance of the compressed joint. The comparison between numerical models of different elements highlights the effectiveness and degree of accuracy of the studied finite element models.

Thus, by concluding with all information and results achieved, it is intended to carry out a study on the Influence of Residual stresses to design of hollow section T-joints which can be used by civil engineers with more reliability and accuracy.

Keywords:

Steel structures, Hollow section Joint, Validation and verification, Residual Stresses

Table of Contents

1. Introduction.....	8
1.1 Hollow Sections and their Joints.....	8
1.2 Residual stresses.....	8
2. State of Art.....	9
2.1 Research on Hollow Section Joints.....	9
2.1.1 Types of Joints.....	10
2.1.2 Design Rules.....	11
2.1.3 Failure Modes.....	13
2.1.4 Welded T Joint between RHS members.....	15
2.1.5 Design resistances of Welded Joints between RHS brace and RHS chord.....	16
2.2 Residual Stresses.....	19
2.2.1 General.....	19
2.2.2 Measurement Techniques.....	20
2.2.3 Influence on Hollow Section Joints.....	21
2.3. Hollow Cold Formed Sections.....	23
2.3.1 Production.....	23
2.3.2 Welding.....	27
2.4 Mechanical Tests.....	28
2.4.1 Specimen design.....	28
2.4.2 Test procedure.....	30
2.4.3 Measurement plan.....	31
3. Objectives.....	32
4. FEA Model.....	33
4.1 Mechanical model.....	33
4.2 Model Without Residual Stresses.....	35
4.2.1 Limit Deformation.....	36
4.2.2. Maximum strain.....	36

4.2.3. Type of structural analysis.....	37
4.2.4. Material properties.....	38
4.2.5. Mesh	39
4.2.6. Support and load conditions	40
4.3 Validation	42
4.4 Verification.....	43
5. Sensitivity Study	44
5.1 Application of Residual Stresses on the model.....	44
5.2 Results and Discussions	46
6. Summary.....	51
6.1 Conclusions	51
6.2 Future Developments	52
References.....	53

1. Introduction

1.1 Hollow Sections and their Joints

A hollow section is a section made up of steel profile having tubular cross section. Hollow sections are available in circular, rectangular, square and elliptical shapes. These hollow sections have same radius of gyration in all directions making it an efficient section. Hollow sections are mostly used in plane and space trusses as they are efficient in compression. Many examples in nature demonstrate the excellent properties of the hollow section as a structural element in resisting compression, tension, bending and torsion forces [4].

According to Eurocode 1993-1-8, Joint is a Zone where two or more members are interconnected. For design purposes it is the assembly of all the basic components required to represent the behaviour during the transfer of the relevant internal forces and moments between the connected members. Normally, Joints in steel structures are usually made by Bolting or welding. Bolting is the most commonly used technique as it is simple and economical. However, welding is deemed in hollow section joints due to its efficiency and aestheticism. Welding has made the connection between the hollow sections easier and resulted in widespread of hollow sections.

European standard EN 1993-1-8, Chapter 7 gives detailed application rules to determine the static resistances of uni-planar and multi-planar joints in lattice structures composed of circular, square or rectangular hollow sections, and of uni-planar joints in lattice structures composed of combinations of hollow sections with open sections [3].

1.2 Residual stresses

Residual stresses are the internal stresses that are remained in an element even after the removal of external loading applied during manufacturing process. Residual stresses were defined in [5] as “locked-in stresses that exist in a body or a part of a body in the absence of any externally applied load”. Steel members are subjected to high temperatures during fabrication by rolling or welding. Cooling of these members always takes place unevenly. Due to this uneven heating and cooling, Structural members contain these residual stresses. Residual stresses are the consequence of several steps in the production of welded structures (manufacturing effects), e.g. the cutting process, the welding process, the assembly process and the cleaning peening [6]. Although it is possible to remove or reduce residual stresses by some mechanical process, it is not recommended in structural engineering applications due to economic reasons.

2. State of Art

2.1 Research on Hollow Section Joints

An extensive research has been performed on the hollow section joints since the evolution of the hollow sections. Hollow sections are being extensively used in structural applications due to their efficiency in resisting compression. However, connecting those hollow sections is important to satisfy the structural needs. Hollow section joint is possible only through welding. The most common welded connections are axially loaded truss type members forming joints in a T, Y or K configurations.

Many design guidelines have been published to design of welded hollow section connections based upon the theoretical and experimental research carried out. First design recommendations for hollow section connections were published forty years ago by International Institute of Welding. Later these recommendations were adopted by many countries around the world. These recommendations have also been included in Eurocode 3.

CIDECT has done an extensive research in the field of hollow section joints. The results of the investigations have been incorporated and updated into the many national and international design recommendations. In 1982, Wardenier [4] published a book “Hollow section joints” in order to establish certain parameters in the design of hollow section joints. The research projects on these joints are still carried out by CIDECT.

Currently in Europe, Design of hollow section joints should be done in accordance with [3] [EN 1993-1-8], Chapter 7: Hollow section joints and CIDECT Design guide for structural hollow sections in mechanical applications.

2.1.1 Types of Joints

The subject of this dissertation concentrates on the uniplanar welded T Joint between the Rectangular hollow sections acting as brace and chord. Most common Uniplanar Hollow section joints are of Y, K, N and T configurations given in Fig.1. These joints are named such because of the resemblance in the shape of respective alphabets.

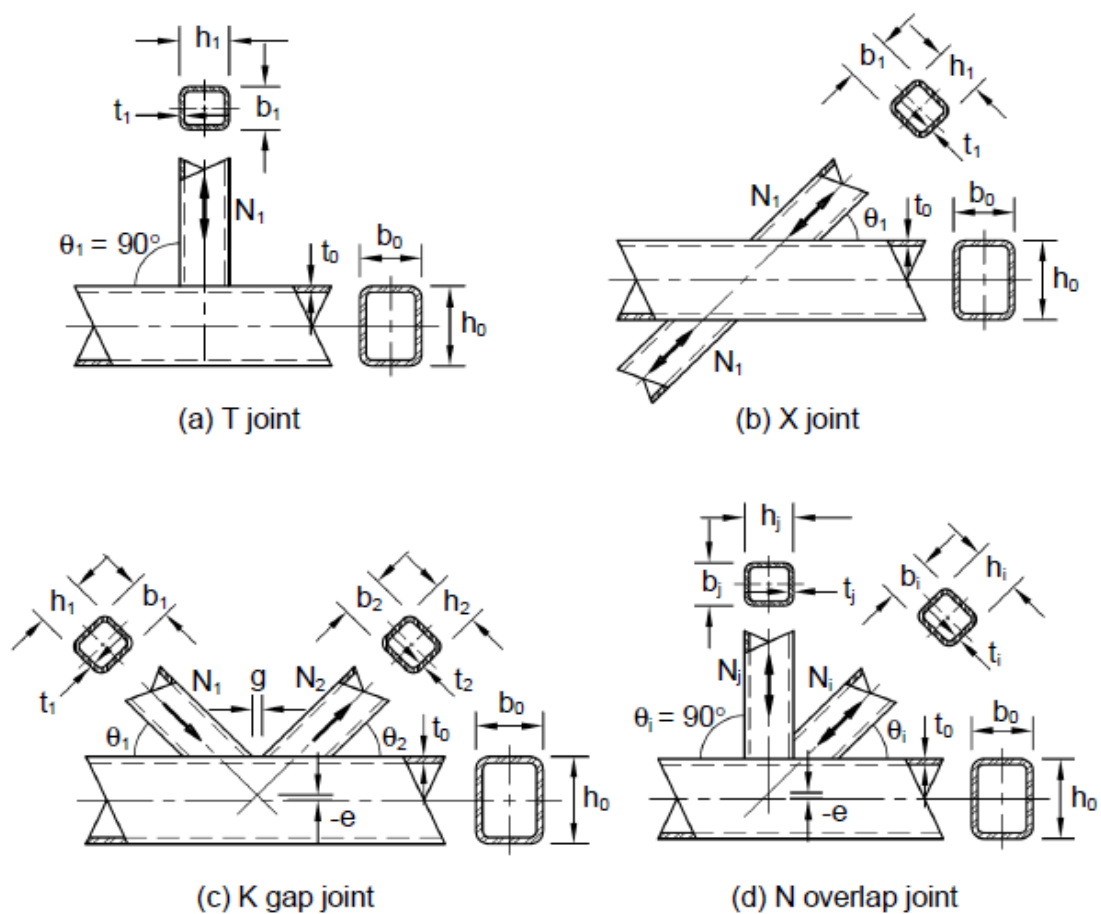


Figure 1 Basic configurations of Hollow Section joints (CIDECT [1])

2.1.2 Design Rules

Eurocode 1993-1-8:2017 [3] specifies that, “For hot finished hollow sections and cold formed hollow sections the nominal yield strength of the end product should not exceed 460 N/mm^2 . For end products with a nominal yield strength higher than 355 N/mm^2 , the static design resistances given in this section should be reduced by a factor 0,9”.

EN 1993-1-8:2017 [3], CIDECT [1] and IIW also states that the nominal wall thickness for any hollow section should not be less than 2.5 mm. Maximum wall thickness should not exceed 25mm unless special measures have been taken to ensure the adequacy of the thickness properties of the material [3].

CIDECT design guide [1] suggests that, for any formula used for computing design resistance, the yield stress should not be considered more than 0.8 times to the nominal ultimate strength.

CIDECT [1] exclusively points out that wall thickness for RHS sections should not be more than 25mm. CIDECT [1] states that the angle between Rectangular hollow sections at the joint should at least be $> 30^\circ$.

EN 1993-1-8:2017 [3] gives range of validity (Table 1) for welded joints between CHS or RHS brace members and RHS chord members.

Table 1 Range of validity for Welded Joints between RHS brace and RHS chord members [EN 1993-1-8:2017, Table 7.10]

		T, Y or X joints	K gap joints
General	General	$\theta_i \geq 30^\circ$ $f_{yi} \leq f_{y0}$ $-0,55 \leq \frac{e}{b_0} \leq 0,25$	$t_i \leq t_0$
		N/A	$0,5(1 - \beta) \leq g/b_0 \leq 1,5(1 - \beta)$ but as minimum $g \geq t_1 + t_2$
	RHS braces	$b_i/b_0 \geq 0,1 + 0,01 b_0/t_0$ but $\geq 0,25$ and $0,5 \leq h_i/b_i \leq 2,0$	
	CHS braces	$d_i/b_0 \geq 0,1 + 0,01 b_0/t_0$ and $0,25 \leq d_i/b_0 \leq 0,80$	
RHS chord	Compression	Class 1 and 2 and $b_0/t_0 \leq 35$ and $h_0/t_0 \leq 35$	
	Tension	$b_0/t_0 \leq 35$ and $h_0/t_0 \leq 35$	
RHS braces	Compression	class 1 and 2 and $b_i/t_i \leq 35$ and $h_i/t_i \leq 35$	
	Tension	$b_i/t_i \leq 35$ and $h_i/t_i \leq 35$	
CHS braces	Compression	Class 1 and 2 and $d_i/t_i \leq 50$	
	Tension	$d_i/t_i \leq 50$	
¹⁾ For $g/b_0 > 1,5(1 - \beta)$, check the K joint also as two separate T or Y joints but with an additional chord shear check in the gap as given in Table 7.14 with $\alpha = 0$.			

2.1.3 Failure Modes

The most economical and common way to connect rectangular hollow sections is by direct connection without any intersecting plates or gussets [7]. The general modes of failures given in Fig.2 and their design rules have been classified based on the numerical and experimental studies of those joints. Modes of failure for RHS have been classified by Wardinier [4] in 1982. Later they were included into EN 1993-1-8, CIDECT [1] and many international design rules. Depending on the type of joint, the joint parameters and the loading conditions several types of failure can occur [4].

According to CIDECT [1], the general modes of failure for uniplanar hollow section joints are,

Mode (a): Plastic failure of the chord face (one brace member pushes the face in, and the other pulls it out)

Mode (b): Punching shear failure of the chord face around a brace member (either compression or tension)

Mode (c): Rupture of the tension brace or its weld, due to an uneven load distribution (also termed “local yielding of the brace”)

Mode (d): Local buckling of the compression brace, due to an uneven load distribution (also termed “local yielding of the brace”)

Mode (e): Shear failure of the chord member in the gap region (for a gapped K joint)

Mode (f): Chord side wall bearing or local buckling failure, under the compression brace

Mode (g): Local buckling of the connecting chord face behind the heel of the tension brace.

To overcome these failures, the welds should be stronger than the connected members and the throat thickness should satisfy the requirements specified in EN 1993-1-8:2017 [7].

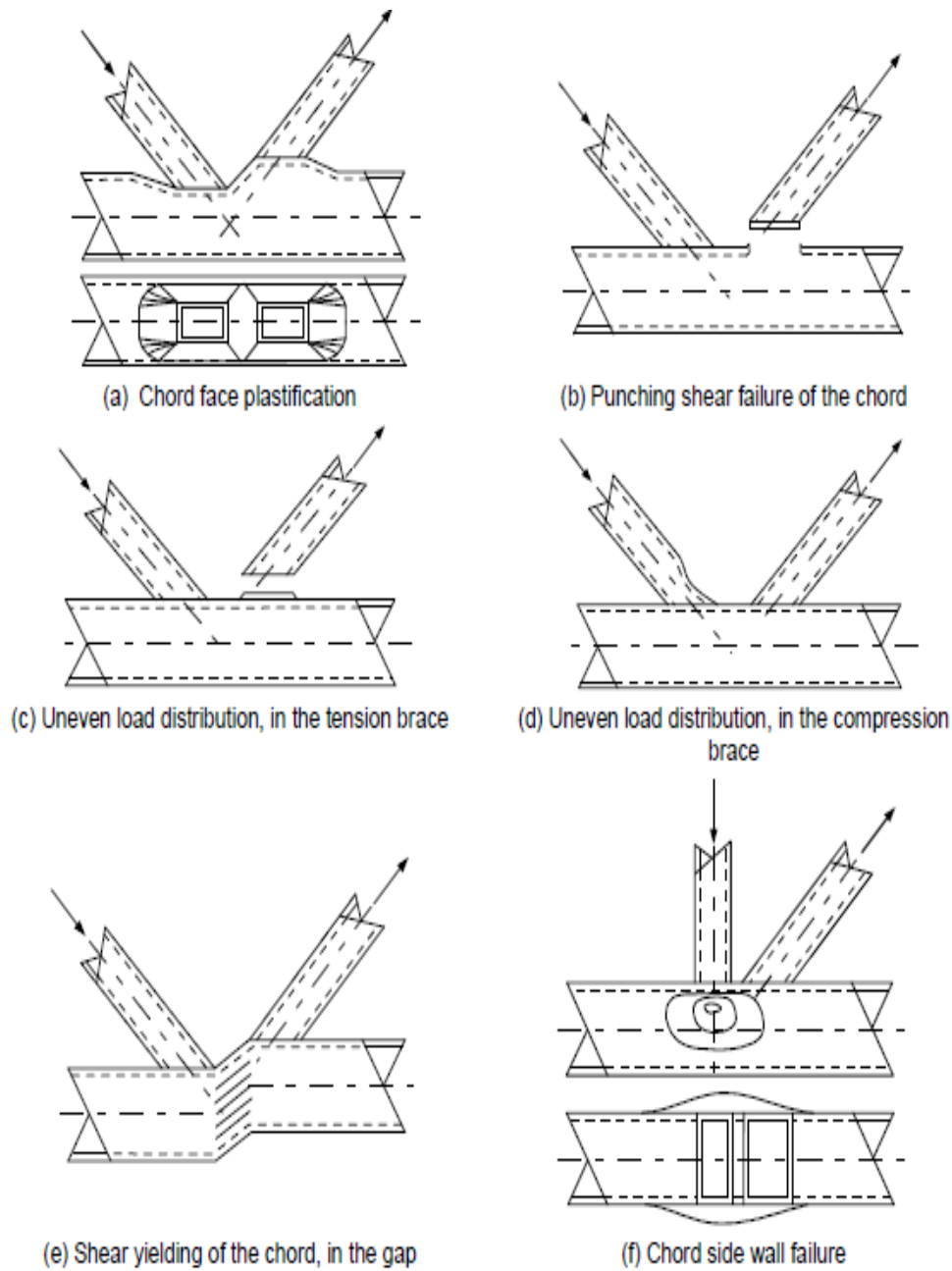


Figure 2 General Modes of failure [1]

2.1.4 Welded T Joint between RHS members

The geometry adopted in this study is a T- Joint “where the horizontal element is the chord, to which the vertical element, the brace, is fully welded. The geometry of a joint is generally defined by the dimensions given in Fig.3 and by the joint parameters $\alpha, \beta, \gamma, \tau$ and g' [7]. In T joint, both the members are connected exactly perpendicular to each other otherwise it is considered as Y Joint. The most common type of joint in hollow sections is the fully welded joint, that is quite simple and aesthetically appealing. One of the reasons for the popularity of this solution is the cumbersome access to the inside of the column, making bolted solutions more complex and costly [12].

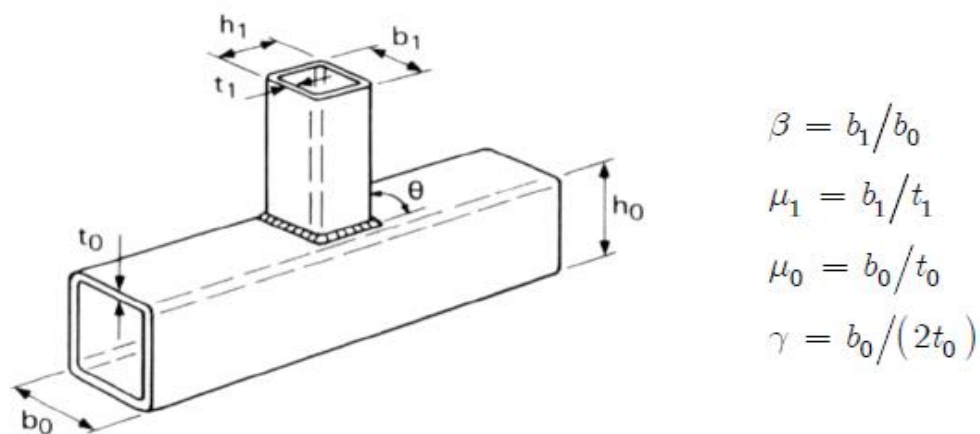


Figure 3 Welded T Joint between RHS brace and RHS Chord

2.1.5 Design resistances of Welded Joints between RHS brace and RHS chord

There are three main failure modes in T joints are, namely web buckling failure, chord flange failure and branch local buckling failure [13]. As our subject mainly deals with T Joint, we will focus on the design resistances for the above-mentioned failures. EN 1993-1-8:2017 [3] provides design formulae given in Table 2 & 3 for the above-mentioned failure modes along with punching shear failure.

Table 2 Design axial resistances for Joints b/w RHS brace and RHS Chord [EN 1993-1-8:2017, Table 7.13]

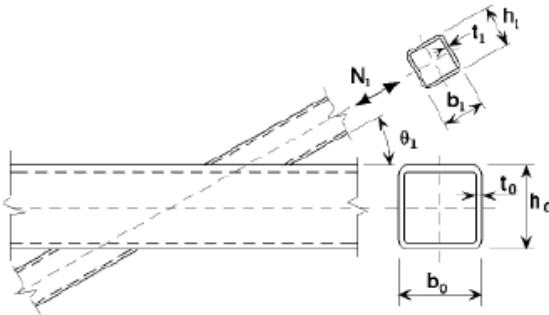
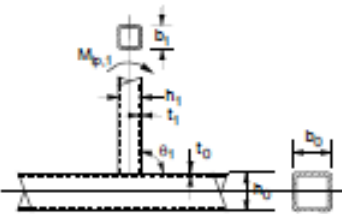
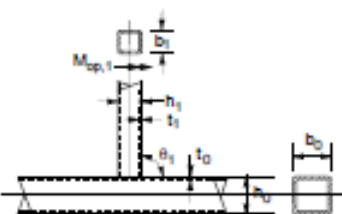
Type of joint	Design resistance ^{1) 2)}
T, Y and X joints	Chord face failure $\beta \leq 0,85$
	$N_{1,Rd} = C_f \frac{f_{y0} t_0^2}{\sin \theta_1} \left(\frac{2\eta}{(1-\beta)\sin \theta_1} + \frac{4}{\sqrt{1-\beta}} \right) Q_f / \gamma_{M5}$
	Chord side wall failure $\beta = 1,0$ ²⁾
	$N_{1,Rd} = \frac{f_b t_0}{\sin \theta_1} \left(\frac{2h_1}{\sin \theta_1} + 10t_0 \right) Q_f / \gamma_{M5}$
	Brace failure
	$N_{1,Rd} = C_f f_{y1} t_1 (2h_1 - 4t_1 + 2b_{eff}) / \gamma_{M5}$
	Punching shear failure $\beta \leq (1 - 1/\gamma)$
	$N_{1,Rd} = C_f \frac{f_{y0} t_0}{\sqrt{3} \sin \theta_1} \left(\frac{2h_1}{\sin \theta_1} + 2b_{e,p} \right) / \gamma_{M5}$
¹⁾ For X joints with $\cos \theta_1 > h_1/h_0$ check the design chord shear resistance using Table 7.14 assuming that $\alpha = 0$.	
²⁾ For $0,85 < \beta < 1,0$ use linear interpolation between the governing resistances at $\beta = 0,85$ (Chord face failure, Brace failure and Punching shear) and $\beta = 1,0$ (Chord side wall failure, Brace failure or Chord shear)	
For circular braces, multiply the above resistances by $\pi/4$, replace b_1 and h_1 by d_1 and replace b_2 and h_2 by d_2 and replace b_{eff} and $b_{e,p}$ by d_{eff} and $d_{e,p}$.	

Table 3 Design moment resistances for Joints b/w RHS brace and RHS Chord [EN 1993-1-8:2017, Table 7.16]

Type of joint	Design resistance		
	Chord face failure (for $\beta \leq 0,85$)		
	$M_{ip,1,Rd} = C_t f_{y0} t_0^2 h_1 \left(\frac{1}{2\eta} + \frac{2}{\sqrt{1-\beta}} + \frac{\eta}{1-\beta} \right) Q_t / \gamma_{M5}$		
	Chord side wall failure ¹⁾ (for $\beta = 1,0$)		
	$M_{ip,1,Rd} = 0,5 f_b t_0 (h_1 + 5t_0)^2 Q_t / \gamma_{M5}$		
	Brace failure (for $0,85 \leq \beta \leq 1,0$)		
	$M_{ip,1,Rd} = C_t f_{y1} \left[W_{pl,1} - \left(1 - \frac{b_{eff}}{b_1} \right) b_1 (h_1 - t_1) t_1 \right] / \gamma_{M5}$		
	Chord face failure (for $\beta \leq 0,85$)		
	$M_{op,1,Rd} = C_t f_{y0} t_0^2 b_1 \left[\frac{h_1(1+\beta)}{2b_1(1-\beta)} + \sqrt{\frac{2(1+\beta)}{\beta(1-\beta)}} \right] Q_t / \gamma_{M5}$		
	Chord side wall failure ¹⁾ (for $\beta = 1,0$)		
	$M_{op,1,Rd} = f_b t_0 (b_0 - t_0) (h_1 + 5t_0) Q_t / \gamma_{M5}$		
	Distortion of the chord due to out-of-plane moments must be prevented		
	Brace failure (for $0,85 \leq \beta \leq 1,0$)		
	$M_{op,1,Rd} = C_t f_{y1} [W_{pl,1} - 0,5t_1(b_1 - b_e)^2] / \gamma_{M5}$		
¹⁾ For $0,85 < \beta < 1,0$, use linear interpolation between the governing resistances at $\beta = 0,85$ (chord face failure and brace failure) and the resistance at $\beta = 1,0$ (brace failure and chord side wall failure).			
Chord stress factor $Q_t = (1 - n)C_1$ according to 7.2.1(3) with $Q_t \geq 0,4$	T, Y and X joints	$C_1 = 0,6 - 0,5\beta$	$C_1 = 0,10$
	K gap joints	$C_1 = 0,5 - 0,5\beta$ but $\geq 0,10$	
Material factor C_t	According to 7.1.1(4)		
Factors b_{eff} and f_b			
$b_{eff} = \left(\frac{10}{b_0/t_0} \right) \left(\frac{f_{y0}t_0}{f_{y1}t_1} \right) b_1$ but $\leq b_1$	Brace in-plane bending	Brace out-of-plane bending	
	T and Y joints	X joints	
	$f_b = \chi f_{y0}$	$f_b = 0,8\chi f_{y0}$	
	where χ is a reduction factor for column buckling, see		

Recently, Sub-commission XV-E of the International Institute of Welding has reanalysed all joint resistance formulae after rigorous experimenting on the RHS joints. New set of recommendations given in Table 4 are provided in CIDECT [1] design guide.

Table 4 Design resistance for Uniplanar joints between RHS brace and RHS chord members [1]

Limit state	Axially loaded uniplanar joints with RHS chord
Chord face plastification (general check for K gap joints; for T, Y and X joints, if $\beta \leq 0.85$)	$N_i^* = Q_u Q_f \frac{f_{y0} t_0^2}{\sin \theta_i}$
Local yielding of brace (general check)	$N_i^* = f_{yi} t_i \ell_{b,eff.}$
Chord punching shear (for $b_1 \leq b_0 - 2t_0$)	$N_i^* = \frac{0.58 f_{y0} t_0}{\sin \theta_i} \ell_{p,eff.}$
Chord shear (general check for K gap joints; for X joints, if $\cos \theta_1 > h_1/h_0$)	$N_i^* = \frac{0.58 f_{y0} A_v}{\sin \theta_i}$ $N_{gap,0}^* = (A_0 - A_v) f_{y0} + A_v f_{y0} \sqrt{1 - \left(\frac{V_{gap,0}}{V_{pl,0}} \right)^2}$
Chord side wall failure (only for T, Y and X joints with $\beta = 1.0$)	$N_i^* = \frac{f_k t_0}{\sin \theta_i} b_w Q_f$

According to CIDECT [1], The parameter Q_u gives the influence function for the parameters β and γ , while the parameter Q_f accounts for the influence of the chord stress on the joint capacity.

For T joints, Q_u and Q_f are calculated by the below given formulae

$$Q_u = \frac{2\eta}{(1-\beta) \sin \theta_1} + \frac{4}{\sqrt{1-\beta}} \quad Q_f = (1-|n|)^{C_1} \text{ with}$$

$$n = \frac{N_0}{N_{pl,0}} + \frac{M_0}{M_{pl,0}} \text{ in connecting face}$$

2.2 Residual Stresses

2.2.1 General

Residual stress is defined as the stress present inside a component or structure after all applied forces have been removed [14]. Residual stresses can be tensile or compressive depending up on the location and type of non-uniform volumetric change taking place due to differential heating and cooling like in welding and heat treatment or localized stresses like in contour rolling, machining and shot peening etc.

According to [14], Residual stresses can be categorized into three types, they are

Type 1: Macro-stresses occurring over a large span that involve many grains within a material.

Type 2: Micro-stresses caused by differences in the microstructure of a material.

Type 3: Exist inside a grain because of crystal imperfections within the grain.

Residual stresses can have a significant effect on the fatigue strength of welded joints and components. Fatigue strength can be increased by compressive residual stresses and can be decreased by tensile residual stresses [6]. Residual stresses, which arise in the welded joints are a consequence of strains caused by solidification, phase change and contraction during welding, also affect the fatigue behavior of welds [9].

Some general effects of Residual Stresses are,

- Low cycle and high cycle fatigue performance
- Distortion
- Peen forming
- Fretting
- Stress corrosion cracking and hydrogen initiated cracking
- Crack initiation and propagation

Presence of residual stresses in the weld joints can encourage or discourage failures due to external loading as their effect is additive in nature. Residual stress can raise or lower the mean stress experienced over a fatigue cycle [14]. It means that mean stress must be controlled properly

according to the type of residual stresses (Compressive or Tensile) to keep the joint unaffected. For this to happen, one need to have a knowledge on measurement of residual stresses.

2.2.2 Measurement Techniques

Measurement of residual stresses is important to evaluate the real behavior of joint. Real data is necessary to improve the accuracy and effectiveness of the finite element modelling. Many measurements of the residual stresses in tubular joints due to the welding process were undertaken by researchers at Cambridge University in the eighties.

For the prediction of the residual stresses and distortions attributed to welding, previous investigations have developed several experimental methods, including stress relaxation, X-Ray diffraction, ultrasonic and cracking [15]. There are many methods of residual stress measurements with varying levels of sophistication and complexity. One of the most simple but effective techniques involves using semi-destructive techniques such as the conventional hole drilling technique and ring-core method [9].

Hole drilling method is based on the stress relaxation induced by the drilling of a small hole: generally, 1-5 mm in diameter and a depth approximately equal to its diameter. Strain-gauge rosettes, glued around the hole before drilling, measure the relieved surface strains. Thus, from these relieved strains, it is possible to calculate the residual stress field present in the material before the hole was drilled [10].

Need for Residual Stress measurements,

- Failures that are suspected as being caused by fatigue, stress corrosion, corrosion fatigue, or hydrogen embrittlement
- Assessment for the continued serviceability of a component
- Distortion occurring during processing of a component
- Distortion of components during storage or in service

2.2.3 Influence on Hollow Section Joints

According to [6], For the study of influence of residual stresses, it is important to know about the factors that influence magnitude and distribution of these stresses. The magnitude and distribution of residual stresses after the finishing of the complete manufacture of the welded structure depend on the material, shape and dimension of the welded structure, the welding process, etc.

Residual stresses, which arise in the welded joints because of strains caused by solidification, phase change and contraction during welding, also affect the fatigue behavior of welds. Tensile residual stress of yield magnitude may exist in as-welded structures and may cause detrimental effects to the fatigue behavior of welded structures [9].

In general, compressive residual stress in the surface of a component is beneficial. It tends to increase fatigue strength and fatigue life, slow crack propagation, and increase resistance to environmentally assisted cracking such as stress corrosion cracking and hydrogen induced cracking. Tensile residual stress in the surface of the component is generally undesirable as it decreases fatigue strength and fatigue life, increases crack propagation and lowers resistance to environmentally assisted cracking.

The above stresses generated in Welded T joint can act in two directions namely transversal and longitudinal to the weld. A stress acting normal to the direction of the weld bead are known as transversal stresses and those acting parallel are known as longitudinal stresses [15].

One of the major conclusions of the research carried out at Cambridge University was that the mean longitudinal stresses (stresses parallel to the weld direction) obtained by sectioning never exceeded the material yield stress, f_y , by more than 20 N/mm^2 . Furthermore, mean transverse residual stresses were never seen to exceed $\sim 0.65 \cdot f_y$. In general, it is the transverse stress distribution that is of the most interest, as the principal stresses due to the applied loads also tend to be oriented perpendicularly (or transversely) to the weld direction [10].

This subject mainly deals with the T joint weld between RHS brace and RHS chord. So, it is important to realize the behaviour of these stresses in this joint. As concluded in [15], very large tensile residual stresses are generated in T joint fillet weld in both transversal and longitudinal direction. These stresses tend to decrease to zero as the distance from weld is increased. Compressive residual stresses are generated only in longitudinal direction of the weld.

Major research on residual stresses [10,11,15] concludes that,

- Compressive residual stresses decrease failure tendency under external tensile stresses primarily due to reduction in net tensile stresses acting on the component.
- Residual stress of the same type as that of external one increases the failure tendency while opposite type of stresses (residual stress and externally applied stress) decrease the same.
- Presence of tensile residual stresses in weld joints causes cracking problems which in turn adversely affect their load carrying capacity.
- Failure of weld joints exposed in corrosion environment is also accelerated in presence of tensile residual stresses by a phenomenon called stress corrosion cracking.

2.3. Hollow Cold Formed Sections

According to [17], the unique feature of cold-formed hollow sections is the magnitude and distribution of residual stress resulting from the cold-forming process. The resulting locked-in residual stress approaches the yield stress of the material and is distributed in a complex fashion both around the section and through the wall thickness. The residual stress measurements do not constitute a comprehensive study into the residual stress in cold-formed hollow sections. However, based upon the work of other researchers on hollow sections the magnitude and distribution of residual stresses due to production and welding are calculated and applied on the studied T-Joint.

2.3.1 Production

Key and Hancock [17] have done an extensive research on the residual stresses in cold formed SHS due to production process. After several experimental and numerical calculations, Magnitude and distribution of residual stresses have been studied and established by the researchers. We have assumed the same pattern of magnitude and distribution on our model.

Based on consideration of forming history and the results of other researchers, representative analytical models have been developed for both the magnitude and distribution of residual stress present in the test specimens. Two stages were involved in the formulation of the residual stress analytical models [17]. These are as follows:

- (1) modelling of the variation of the residual stress through the section wall thickness; and
- (2) specification of the magnitude and distribution of residual stress around the cross-section.

These stresses are detailed below including the final residual stress model due to cold forming process

The following steps were taken to analytically model the residual stress variation through the wall thickness:

- (1) The panel removal residual stress was modelled as a membrane component and a bending component, as shown in Figs 14 and 15 for the longitudinal and transverse directions, respectively.
- (2) The released residual stress determined from small block removal was negligible compared with the panel removal stress and was ignored for the analytical modelling.
- (3) The released residual stress determined from layering were modelled for the longitudinal and transverse directions respectively. The analytical models satisfy the equilibrium requirement of

zero net axial force and moment. Thirteen-layer points were used in the finite strip analysis to adequately model the residual stress distribution through the wall thickness. These layer points, labelled P~ to P13, are also shown in Figs 4 and 5.

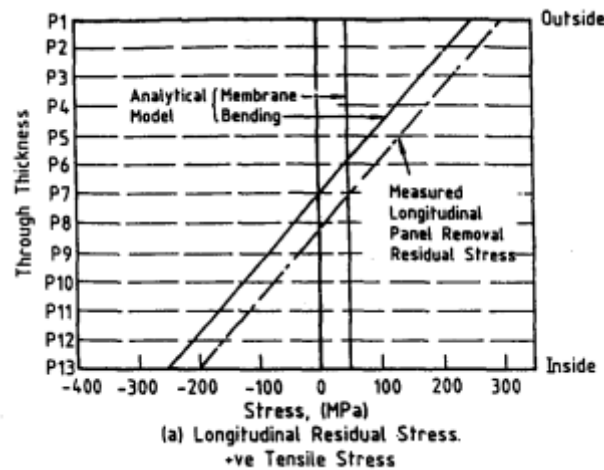


Figure 4 Analytical model for Longitudinal Residual stresses

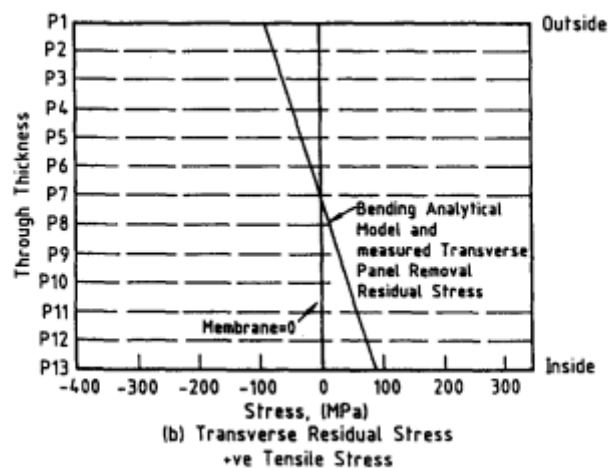


Figure 5 Analytical Model for Transverse Residual stresses

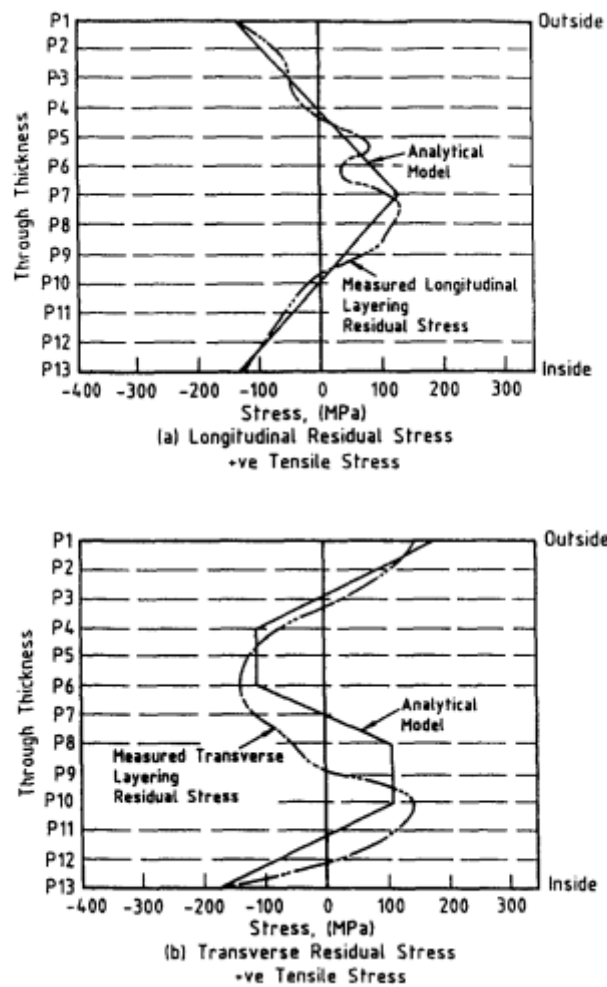


Figure 6 Analytical model of layering residual stress

For the studied Joint, Residual stresses due to production are applied only on 5-layer points using *INITIAL CONDITIONS, TYPE=STRESS, SECTION POINTS command in Abaqus. The layer points that are selected for application of Residual stresses are P1, P4, P7, P10 and P13 respectively.

According to Key and Hancock [17], Following pattern on residual stresses are applicable for the RHS,

- Longitudinal membrane component, σ_R , equal to $\chi\sigma_R$, where σ_R is 30 MPa and χ is the distribution on each face given by Fig. 7(a).
- Longitudinal bending component, σ_{Rlb} , equal to $\chi\sigma_R$, where σ_R is the analytical bending variation shown in Fig. 4 and χ is the distribution on each face given by Fig. 7(b).
- Longitudinal layering component, σ_{Rll} , equal to $\chi\sigma_R$, where σ_R is the analytical layering variation shown in Fig. 6(a) and χ is the distribution on each face given by Fig. 7(c).

- Transverse membrane component is zero.
- Transverse bending component, σ_{Rtb} , equal to $\chi\sigma_R$, where σ_R is the analytical bending variation shown in Fig. 5 and χ is the distribution on each face given by Fig. 7(e).
- Transverse layering component, σ_{Rtl} , equal to $\chi\sigma_R$, where σ_R is the analytical layering variation shown in Fig. 6(b) and χ is the distribution on each face given by Fig. 7(f)

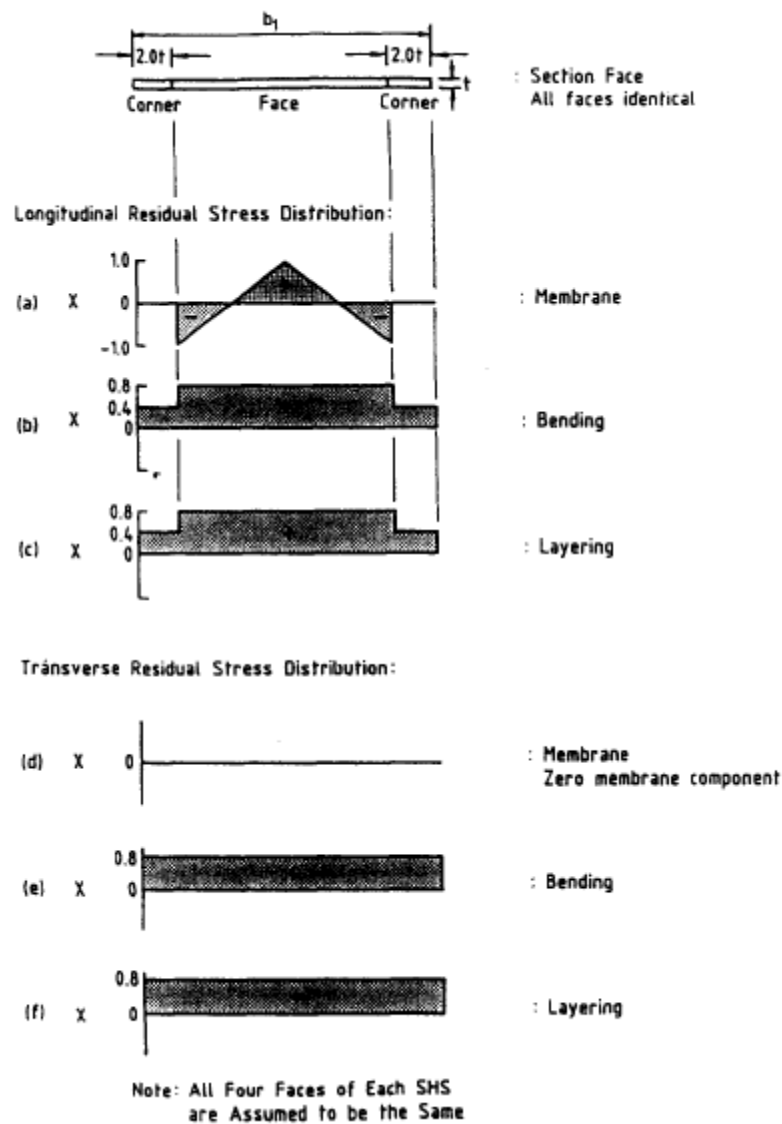


Figure 7 Analytical models of residual stress distribution across section face [17]

According to M. Jandera and J. Machacek [16], Residual longitudinal membrane stresses in corners were always calculated from the condition of equilibrium over the whole cross-section. Their magnitudes were very low. The variation of resistance results principally from the effect of residual bending stresses on the non-linearity of the stress-strain curve. So, membrane component is ignored in our study and only bending component along with layering component is considered.

2.3.2 Welding

Welding residual stress field is important for the function of the structure as it may influence the mechanical behaviour of structures including their fracture, stress corrosion cracking, fatigue, and buckling characteristics. Tensile residual stresses are detrimental to the initiation and growth of fatigue cracks [22]. Acevedo and Nussbaumer [10] studied results of experimental residual stress measurements by different techniques and a distribution function is proposed for the critical transverse residual stress field in the weld toe vicinity. Transverse residual stresses are of most interest in fatigue assessment since they superimpose with principal applied stresses. We have considered the same distribution functions shown in Fig.8 proposed in [10] for our studied joint.

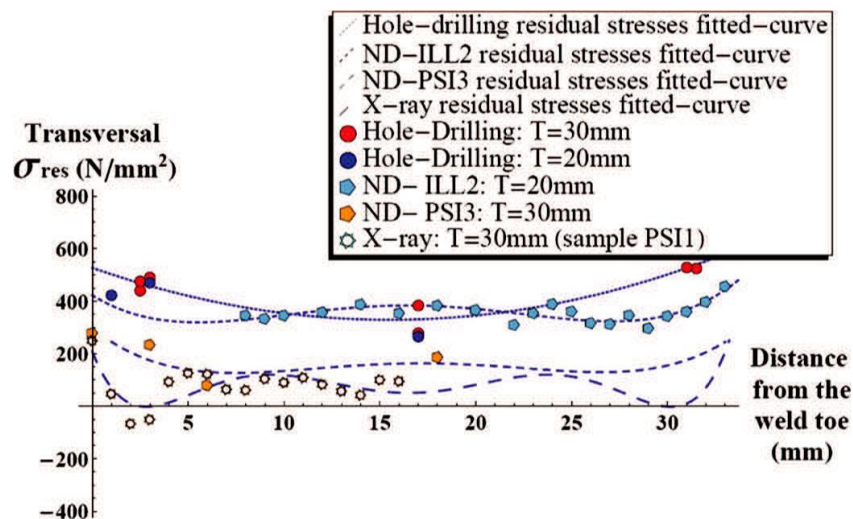


Figure 8 Residual stresses pattern measured by different techniques [10]

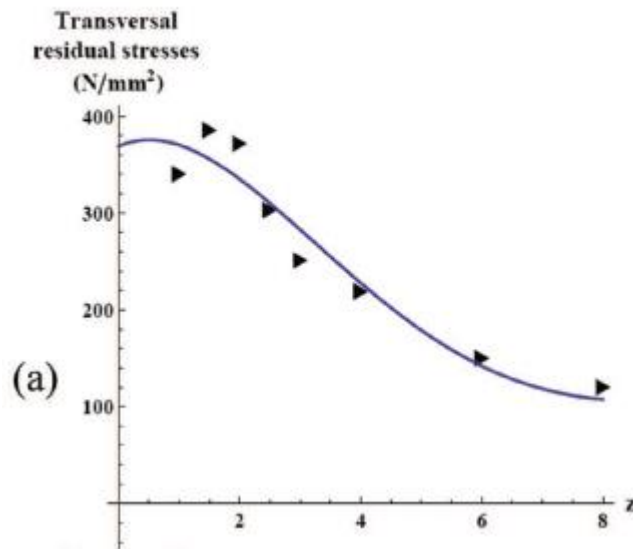


Figure 9 Transversal Residual Stress distribution through thickness [10]

2.4 Mechanical Tests

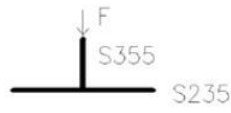
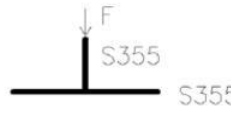
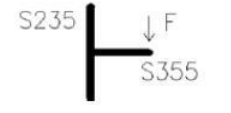
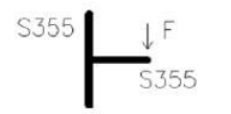
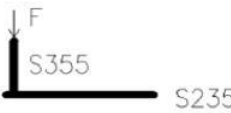
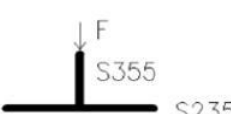
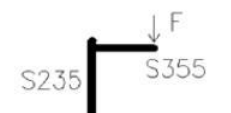

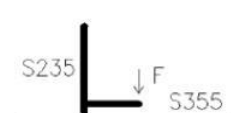
2.4.1 Specimen design

A series of experiments on the hollow section T-joint were performed at the laboratory of the steel and timber structures department of the Czech Technical University in Prague.

For these experiments, a total of 9 RHS brace-RHS chord T-joints specimens made of steel were designed as shown on Figure 8 - Experiment specimen 2.02. E.Sy.Co.235. The strain distribution and vertical displacement were measured, failure modes of joints were observed, and finally ultimate axial compressive capacity was derived. Dimensions of the specimen are summarized on Figure 12. The schematic diagrams of specimens are shown in Table 5 - Schematic Load Application

At the top of the brace, an end plate was welded to uniformly transmit the axial load to the brace section.

Table 5 Scheme of Load Application

Name of specimen	Number of drawing	Steel grade		Sketch
		chord	brace	
1.01.T.Ec.Co.235	42012	S235	S355	
1.02.T.Ec.Co.355	42015	S355	S355	
1.03.T.Ec.Be.235	42017	S235	S355	
1.04.T.Ec.Be.355	42016	S355	S355	
2.01.E.Sy.Co.235	42008	S235	S355	
2.02.E.Sy.Co.235	42011	S235	S355	
2.03.E.Sy.Be.235	42001	S235	S355	
2.04.E.Sy.Be.235	42006	S235	S355	
2.05.E.Sy.Be.235	42007	S235	S355	

2.4.2 Test procedure

All specimens were installed in the same loading setup as shown in Figure 10 - Experiment loading setup. During the experimental tests, the bottom flange of the hollow section steel chord was fixed in all directions and an axial compressive load was applied at the top end of the brace. Axial loads were applied at the loading plate by a hydraulic jack and are monitored by a load cell positioned concentrically between the jack and the reaction frame

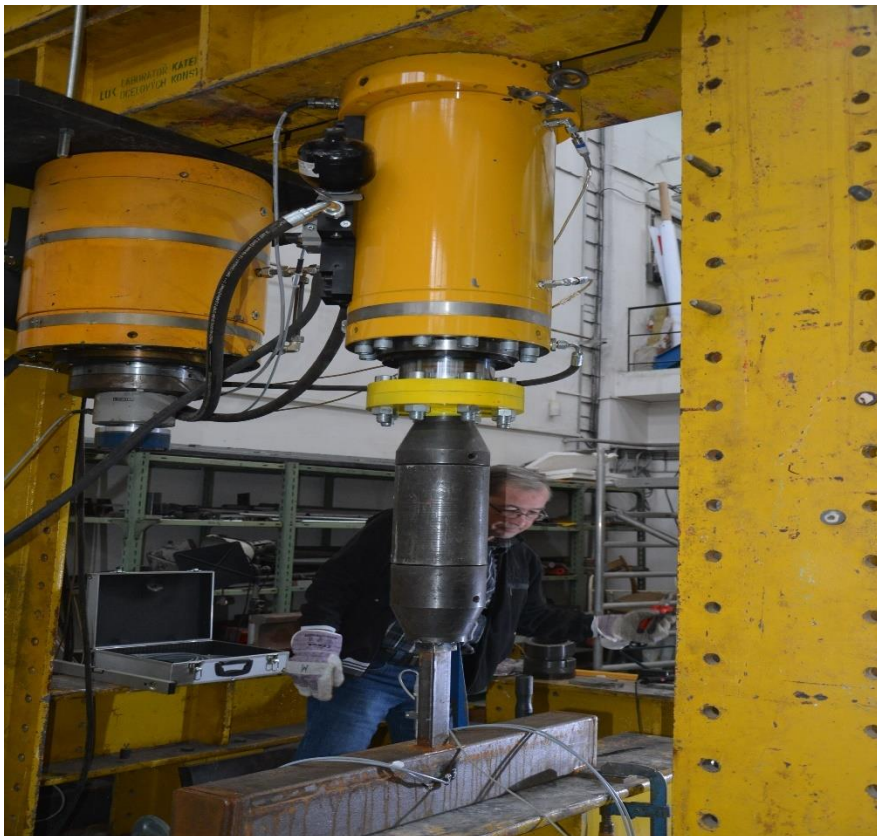


Figure 10 Experiment loading setup

2.4.3 Measurement plan

To obtain the necessary information for the analysis, the test plan consisted of two measurement devices:

- (1) Strain gauges.
- (2) Potentiometers

To capture the strain in each test is a difficult task, which can only be achieved through the utilization of well positioned strain gauges. The strain gauges were positioned approximately at the areas where the strains increase first, and the failure occurs. This means that strain gauges were placed at both vertical faces of chord and foot of the brace as shown in Fig.11, to obtain strain intensity distribution. In total 4 strain gauges were placed for each experiment.



Figure 11 Strain gauge placement

3. Objectives

Design rules for joints between hollow sections are based on simple theoretical mechanical models and they are fitted through comparisons with experimental tests. Nowadays, numerical models are becoming an important tool for designing connections with accuracy and reliability, and the present study intends to explore this field.

The primary goal for this dissertation is to study the influence of Residual stresses on the design resistance of hollow section joints.

To achieve the primary goal, following objectives are to be achieved

- Extensive study on Residual stresses and their influence in steel structural members
- Study on the hollow section joints and their failure modes.
- Creation of shell and solid element numerical models with the use of software ABAQUS by using the same parameters as experimental data.
- Application of different pattern and magnitude of Residual stresses on the numerical models.
- Validation and verification of numerical models by comparing outputs of numerical models to experimental and analytical results
- Perform sensitivity tests on numerical models by changing geometric parameters to understand better the strength behavior and failure modes of the T-joint.
- Investigate analysis results to see the influence of Residual stresses on design resistance and behavior of hollow section joints.

4. FEA Model

4.1 Mechanical model

We have considered Experiment specimen 2.02. E.Sy.Co.235. for this study and the validation and verification is done to the results of this specimen in the chapter 3.

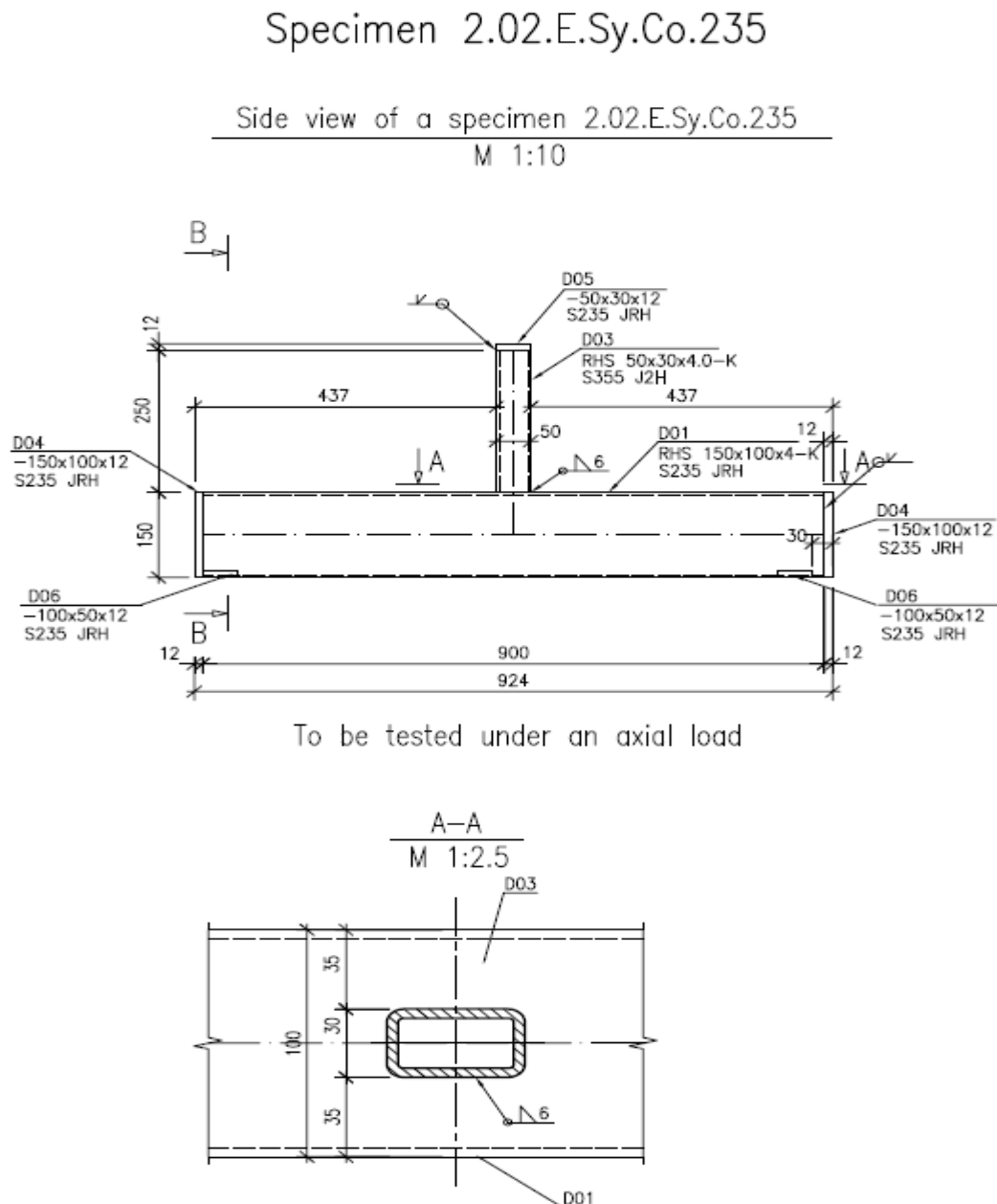


Figure 12 T-Joint model considered in this study 2.02. E.Sy.Co.235

Chord Face Failure is seen as shown in Fig.13 in all the specimens tested in mechanical tests for Compressive load from top of the brace.



Figure 13 Deformed shape of the Specimen

4.2 Model Without Residual Stresses

The latest research progress and commercial finite element codes are capable to simulate almost all complex phenomena affecting the connection response (three-dimensional behavior, combined nonlinear phenomena like material and geometrical nonlinearities, friction, slippage, contact, Weld interaction and fracture). However, still difficulties remain to the numerical analyst which must choose appropriate finite element models able to provide an accurate representation of the physics with the lowest computational cost. Choice of the mesh, node number, integration point number through the element thickness and time-step size for constitutive law integration depend upon resources, geometry, type of loading and required accuracy.

The software ABAQUS was used in the present study to model the hollow section T-joint. By using ABAQUS 3D solid and shell elements, members of the joint could be modeled as a sharp notch given in Fig.14. This software allowed us to apply residual stresses and it can produce accurate and detailed stress distribution near the intersection of member and results will be later discussed on this study.

ELEMENT TYPE AND SIZE	MATERIAL
CHORD 150X100X4	S235
BRACE 50X30X4	S355

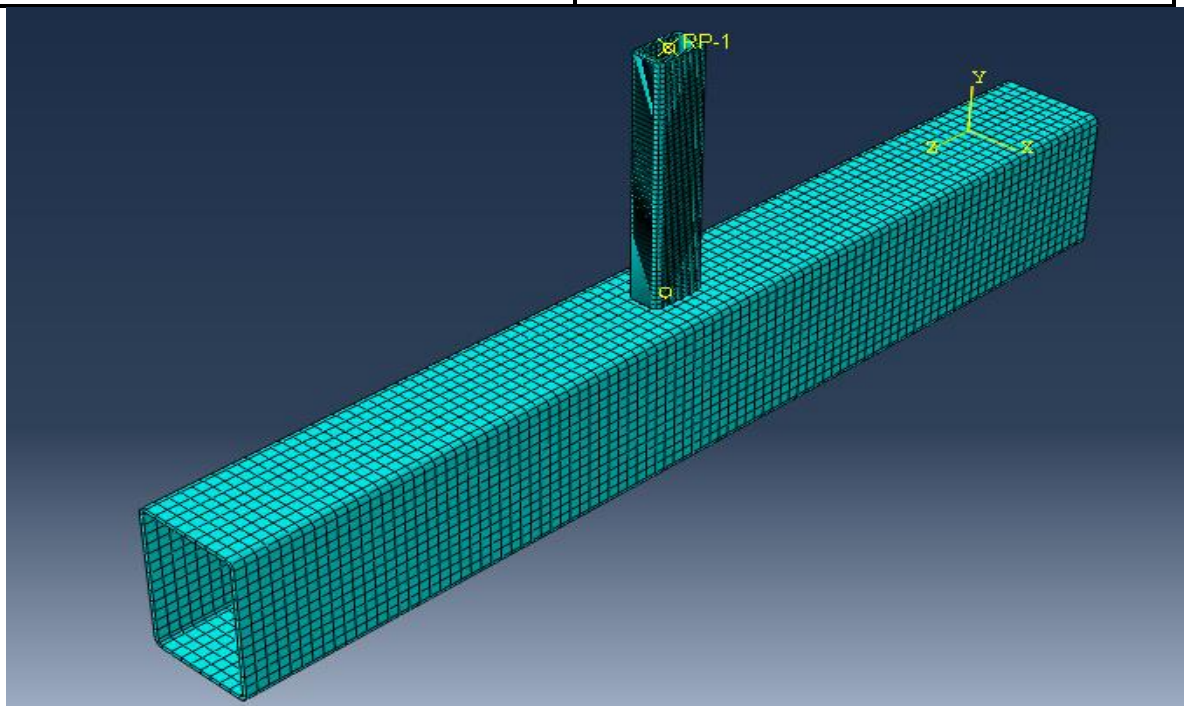


Figure 14 FE model of RHS T-Joint

4.2.1 Limit Deformation

According to Wardenier [7], joint design is based on the limit state (or states), corresponding to the “maximum load carrying capacity”. The latter is defined by criteria adopted by the IIW Sub-commission XV-E [18], namely the lower of:

- (a) The ultimate strength of the joint, and
- (b) The load corresponding to an ultimate deformation limit.

An out-of-plane deformation of the corresponding RHS face, equal to 3% of the RHS connecting face width ($0,03b_0$), is generally used as the ultimate deformation limit [19] in (b) above. This serves to control joint deformations at both the factored and service load levels, which is often necessary because of the high flexibility of some RHS joints. In general, this ultimate deformation limit also restricts joint service load deformations to $\leq 0,01b_0$. Wardenier et al. wrote [7] that, some design provisions for RHS joints are based on experiments undertaken in the 70’s, prior to the introduction of this deformation limit and where ultimate deformations may have exceeded $0,03b_0$. However, such design formulae have proved to be satisfactory in practice.

Also, according to Chen & Wu, for the deformation curves of SHS brace-H-shaped steel chord T-joints with no distinct peaks and a drop load, the joint strength F 3% of b_0 at the deformation of 3% of the chord width (b_0), was a failure load. But, for Chen & Wu experiments, the deformation of all axially loaded T-joints was less than 3% of b_0 . For this, the ultimate limit state was the last criterion used to define failure in the joints. So, the useful experimental data was obtained before specimens suddenly buckling failure, and the top point of curve was defined as ultimate capacity.

4.2.2. Maximum strain

For the failure modes of the FE models, it was taken into consideration the limit state criteria according to EN 1993 1-5 cl. C.8 (1) [3], “*the national annex may specify the limiting of principal strain. A value of 5% is recommended.*” This means that a failure mode is reached once any part of the specimen reaches the strain of 5%.

4.2.3. Type of structural analysis

The type of analysis chosen in ABAQUS to assess the hollow section T-Joint was the static, Riks method. This method is generally used to predict unstable, geometrically nonlinear collapse of a structure.

The constitutive model is integrated by means of the explicit forward Euler algorithm. To determine the structural response of the nonlinear problem, an implicit solution strategy is used. Hence, a load stepping is used. The increment size follows from accuracy and convergence criteria. Within each increment, the equilibrium equations are solved by means of the Newton-Raphson iteration [20].

In the end of each load increment, or group of increments, the coordinates of the structure are updated to the deformed configuration. In the next increment, these coordinates start to belong to an “undisturbed” configuration and the stresses already installed due to the previous increments are treated as initial stresses referent to a deformation equal to zero. This process goes on, increment by increment, until the end of the analysis. In finite elements, the mesh keeps connected to the integration points during all the process if the correct features are applied. The load increments are intervals of loads, useful in a way that it allows to analyze the joint behavior in a restrict number of intervals demanded by the user, according to the joint to be analyzed and regarding the deformation capacity of the material. Thus, as the applied loads on the joint are slowly enough, it is acceptable to consider the inertia forces negligible and a static analysis on the joint can be used [21].

Considering all these above referred aspects, the type of analysis considered in the numerical modelling is a static analysis with an elastic-plastic steel behaviour.

4.2.4. Material properties

According to [21], steel is the material of the specimens. As an isotropic material, the steel used has the same characteristics in all directions, which means that has symmetrical characteristics in relation to one arbitrary orientation plane.

The bilinear material model in ABAQUS library was used in the finite element analysis. The initial part of the bilinear curve represents the elastic property up to tensile yield stress (f_y), with measured elastic modulus (E) and Poisson's ratio (ν). The post-yield response of the bilinear material model was developed based on the measured ultimate tensile stress (f_u) and elongation [38].

The characteristic material properties are assumed, according to EN 1993 1-1 [2]:

Table 6 Nominal values for Yield strength and Ultimate strength [2]

Standard and steel grade	Nominal thickness of the element t [mm]			
	t ≤ 40 mm		40 mm < t ≤ 80 mm	
	f_y [N/mm ²]	f_u [N/mm ²]	f_y [N/mm ²]	f_u [N/mm ²]
EN 10025-2				
S 235	235	360	215	360
S 275	275	430	255	410
S 355	355	510	335	470
S 450	440	550	410	550

The strains are calculated by using the following formulae given in Table 7:

Table 7 Strain calculation example

Stress (MPa)	Strains	
0	0	0
$F_y = 355$ MPa	$\varepsilon_1 = \frac{F_y}{E}$	0.00169
$F_y = 355$ MPa	$\varepsilon_2 = 0,025 - 5 \cdot \frac{F_u}{E}$	0.01286
$F_u = 510$ MPa	$\varepsilon_2 = 0,02 + 50 \cdot \frac{F_u - F_y}{E}$	0.05690
$F_u = 510$ MPa	∞	0.20

4.2.5. Mesh

The finite element mesh stands for one of the most important aspects for an accurate result in a numerical simulation. A finer finite element mesh usually gives better calculation results. However, as a mesh is made finer, the computation time and cost increases. A finer mesh depends on many factors. Among them is the cost versus the accuracy to receive. The cost increases with the number of DOF's.

The mesh density required can be a function of many factors. Among them are the stress gradients, the type of loadings, the boundary conditions, the element types used, the element shapes, and the degree of accuracy desired.

The type of the mesh elements (quadratic or triangular) also play an important role to consider for the refinement process, being necessary for such process, to have in consideration the shape of the mesh for the structural elements (undistorted or distorted).

It is important to keep the elements with an appropriate aspect ratio. Also, elements must not cross interference to be able to capture the higher stress concentration which occurs on those areas. The good practice also tells that is preferable to use quadrilateral over triangles for 2D models, and bricks over wedges and tetrahedral for 3D models.

Distortion of the element should be taken into consideration when meshing a model. For this study, it was chosen quadratic elements with four nodes for shell elements and 3D elements containing 8 nodes for solid elements. Ideal size of the mesh should be a result of a convergence study to combine higher accuracy of the results and lower time/cost of the computational processing.

The stiffness, mass and volume of an element are calculating numerically through the called "integration points". These points influence the element's behavior, which can be analyzed by a full or reduced integration. The difference between these types of integration is on the number of points needed to integrate the polynomials of the matrices required to develop the finite element method.

4.2.6. Support and load conditions

Support and load conditions were applied to the FE models according to the tests. Loads were applied at the top of the brace and, to recreate the same condition on the models, a reference point was created at the center of the brace at top. Rigid couplings to the brace's edges were implemented, as show on Figure 15 - Load point coupling to top of braces edges. On this reference point the different loads were applied to obtain similar conditions to the experiments and to ensure a convenient numerical analysis.

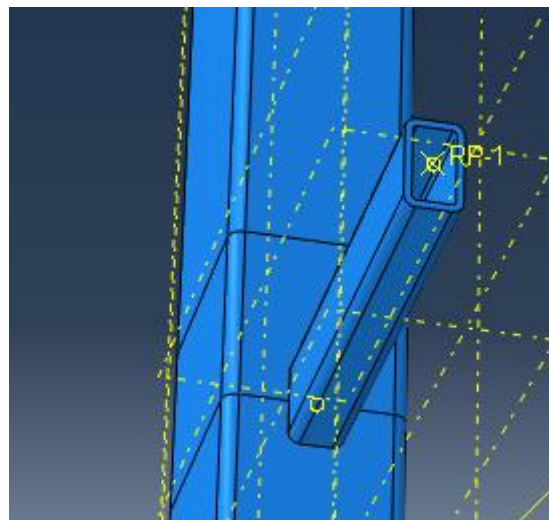


Figure 15 Load point coupling to top of braces edges

Boundary conditions were applied to the bottom flange of the chord (rotation and translation restrain on all axis) to recreate the same conditions as the experiments (Fig.16).



Figure 16 Specimen 2.02. E.Sy.Co.235 -Before the test

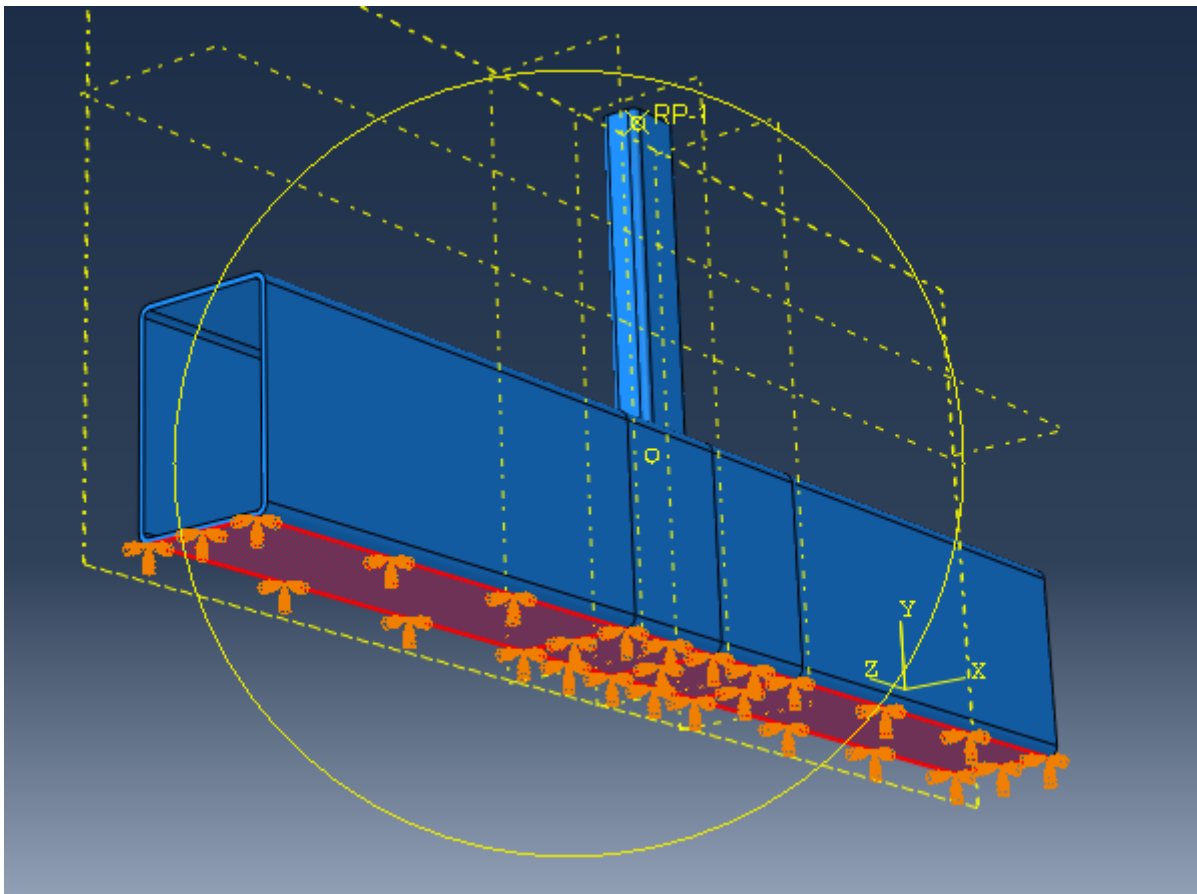


Figure 17 Bottom flange boundary conditions

The interface between the top flange of the chord and bottom section of the brace was modeled by using a contact interaction on ABAQUS as shown in Fig.17. An analytic rigid contact interaction was established by using a “master-slave” algorithm available in the ABAQUS library. The contact interaction allows the surfaces to separate under the effect of tensile forces. However, they are not allowed to penetrate each other under the effect of compressive loadings.

4.3 Validation

Results achieved by performing simulations on FEM software can only be proved to be correct by a methodical validation and verification procedures. This procedure is important for the analysis since it guarantees the results to allow the right assessment for the decision making.

The validation process was performed through simulations of the elastic-plastic behavior of realistic T-joint connections between RHS profile (brace) and RHS profile (chord), to the ultimate limit state. The comparison between numerical analysis and reference values (experimental data) in each phase made it possible to demonstrate the high accuracy and effectiveness of the proposed finite elements models as shown in Fig.18.

For the validation, Research Oriented FEM was built by using solid elements. Influence of the element size, number of elements through thickness on chord and brace, mesh convergence study and the stress-strain diagram obtained from experimental data were investigated as a part of the validation.

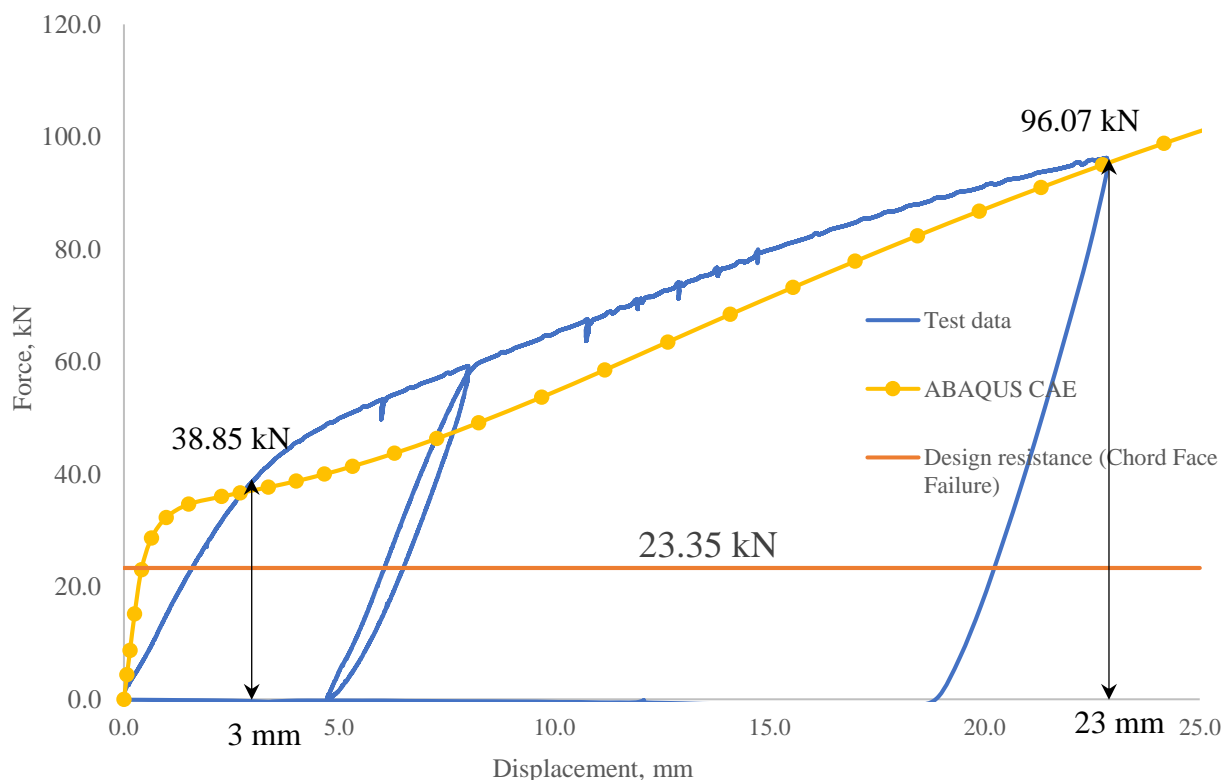


Figure 18 Validation of Numerical model with Experimental data

4.4 Verification

For the verification, Research oriented FEM was built using shell elements(S4R). This model is verified by comparing with both numerical model from solid elements and with the reference values (Experimental data). To apply Residual stresses due to cold forming process, this model is chosen because of its flexibility to apply stresses in layers across the thickness.

Results of the analyses obtained from validated numerical models were compared to experimental data in Table 8.

Table 8 Comparison of Resistance between Experimental data and Numerical data

Model	Resistance at 3% of b_o (3mm)	Ultimate Resistance
Experimental data	38.85 kN	96.07 kN
Numerical Model Solid	25.96 kN	96.72 kN
Numerical Model Shell	22.16 kN	96.78 kN

5. Sensitivity Study

5.1 Application of Residual Stresses on the model

In this study, Exclusive study was performed on the rectangular hollow section T-Joint. RHS 150x100x4 as a chord and 50x30x4 as brace were used for modelling. The bilinear material model of steel including the elastic modulus (E) OF 205 GPa, tensile yield stress of 355 MPa for brace and 235 MPa for chord and Poisson's ratio (ν) of 0,3 were used in the study. For the deformation curves of the joints with clear peak load, the peak load was used as the failure load, which occurs in all cases (Chord Face Failure).

Two different models were created in Abaqus using solid(C3D20) and shell(S4) elements as show in Fig.19 & 20 respectively. For the verification, shell element model was used. It is well known that in comparison to solid elements, shell elements give less accurate results. However, when it comes to the development and time process of the model, it is simple and quicker to make, which can be handful for structural engineers. But, in all cases, inputs must be carefully taken into consideration, knowing that it is common to have as results for shell FEM higher resistance than analytical and experimental solutions, as it will be showed on this study.

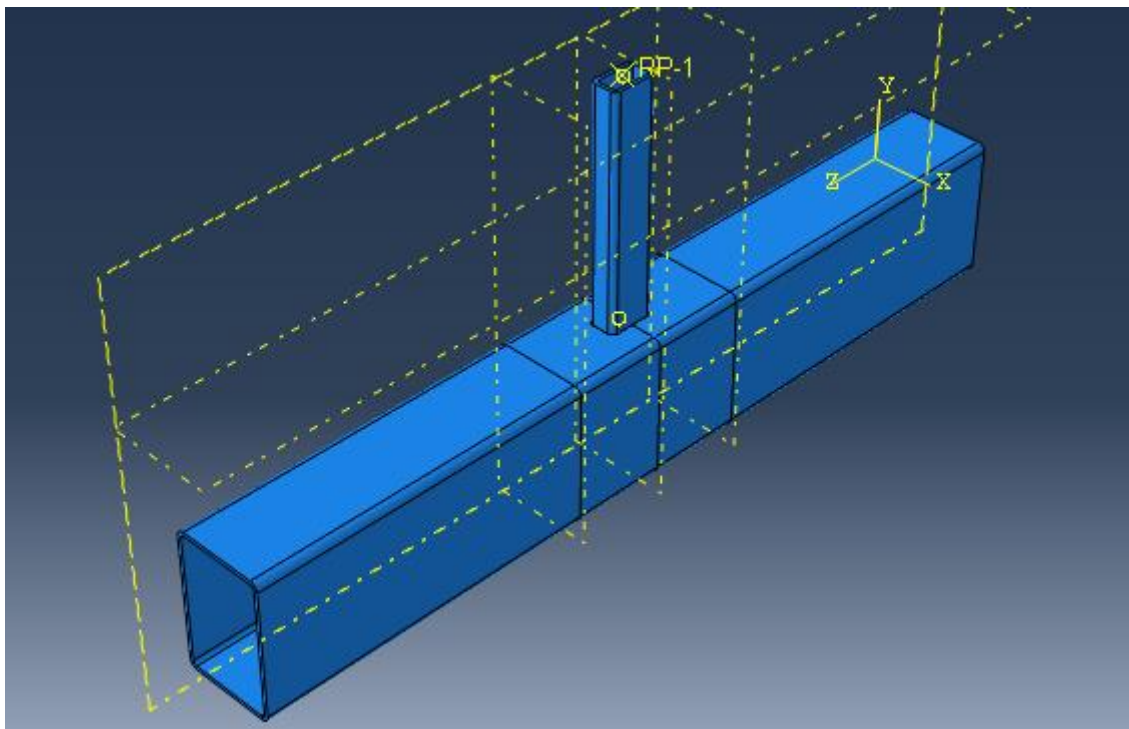


Figure 19 FEM model with solid elements

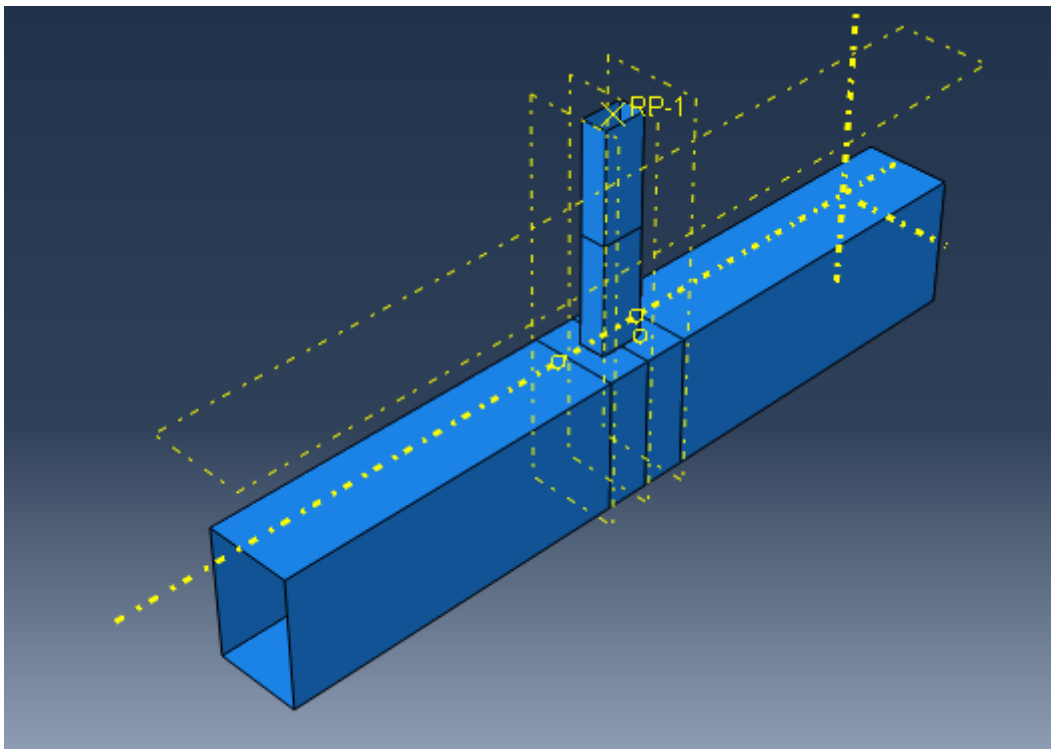


Figure 20 FEM model with shell elements

5.2 Results and Discussions

Welding Residual stresses in Abaqus were introduced using “*INITIAL CONDITIOS, TYPE=STRESS” for solid element model. Both production and welding Residual stresses were introduced in shell element model in layers as discussed in chapter 4 using “INITIAL CONDITIONS, TYPE=STRESS, SECTION POINTS”. Solid model didn’t allow us to apply residual stresses in layers. So, Shell element model was created and verified with solid element model before applying residual stresses. Convergence of the plots is discussed in the chapter.4

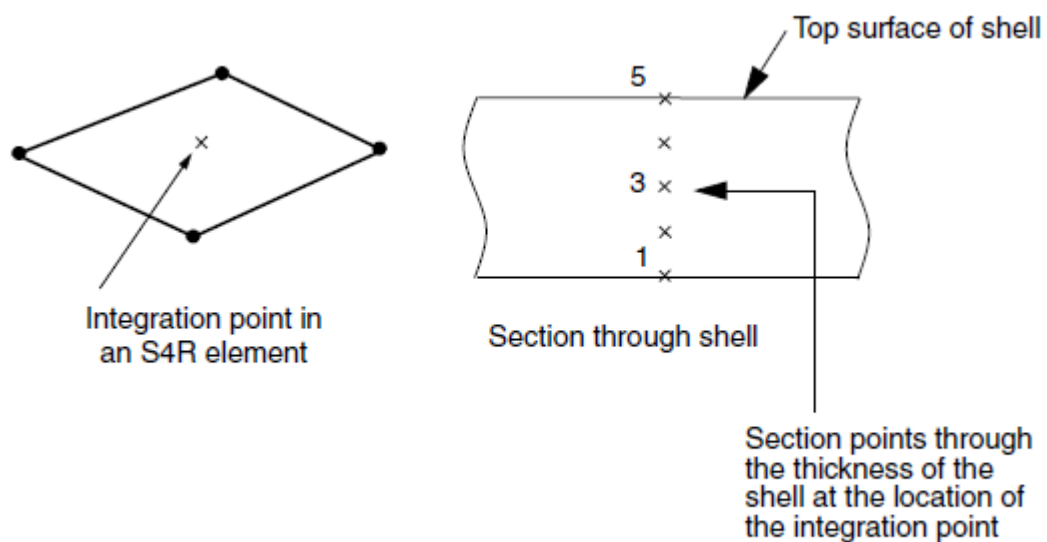


Figure 21 Configuration of section points in a numerically integrated shell [23]

This dissertation main objective is to study the influence of residual stresses on the resistance of hollow section joints. A model with solid element was created and subjected to compressive loading on top of the brace. Force vs Displacement graphs were drawn before applying residual stresses and validated with the experimental results that are carried out at Czech Technical University in Prague as mentioned in Chapter 2. Chord face failure is seen in the numerical models also as shown in Fig.22.

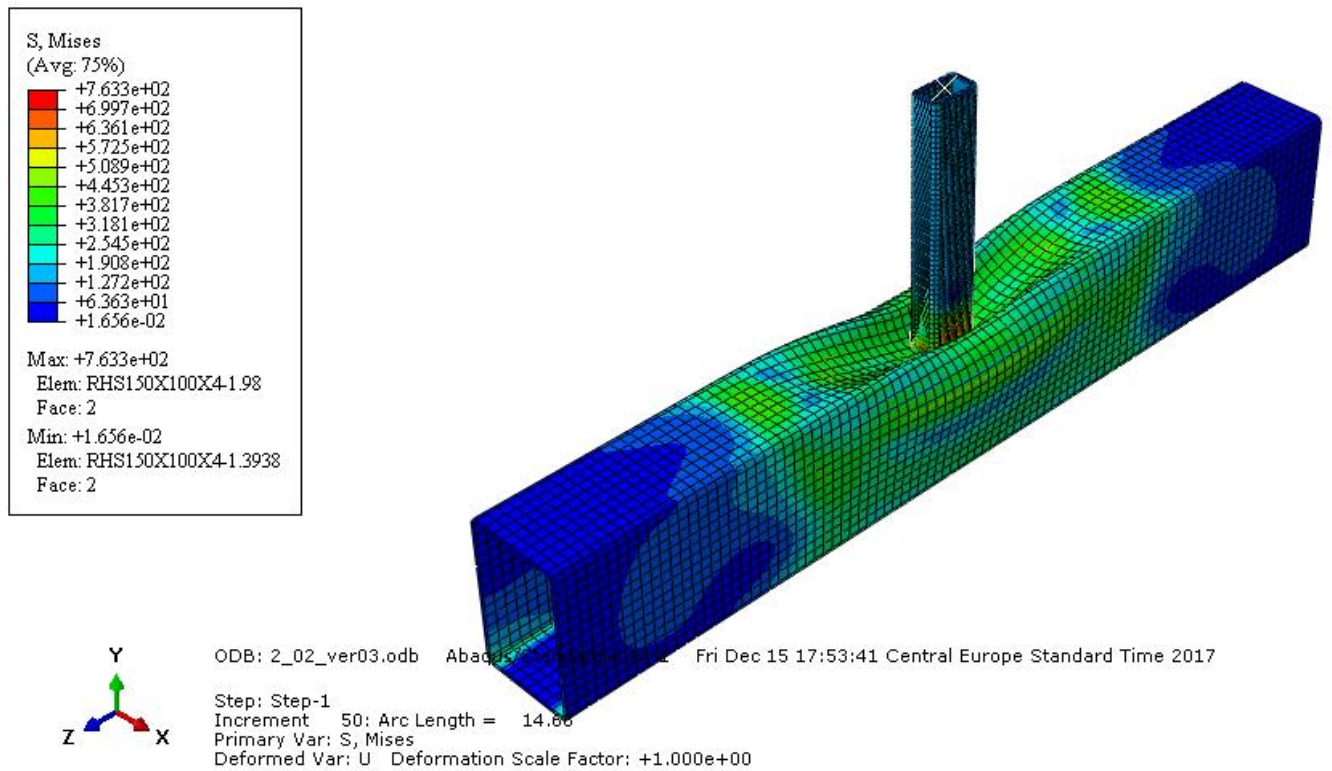


Figure 22 Deformed Shape of the Numerical model

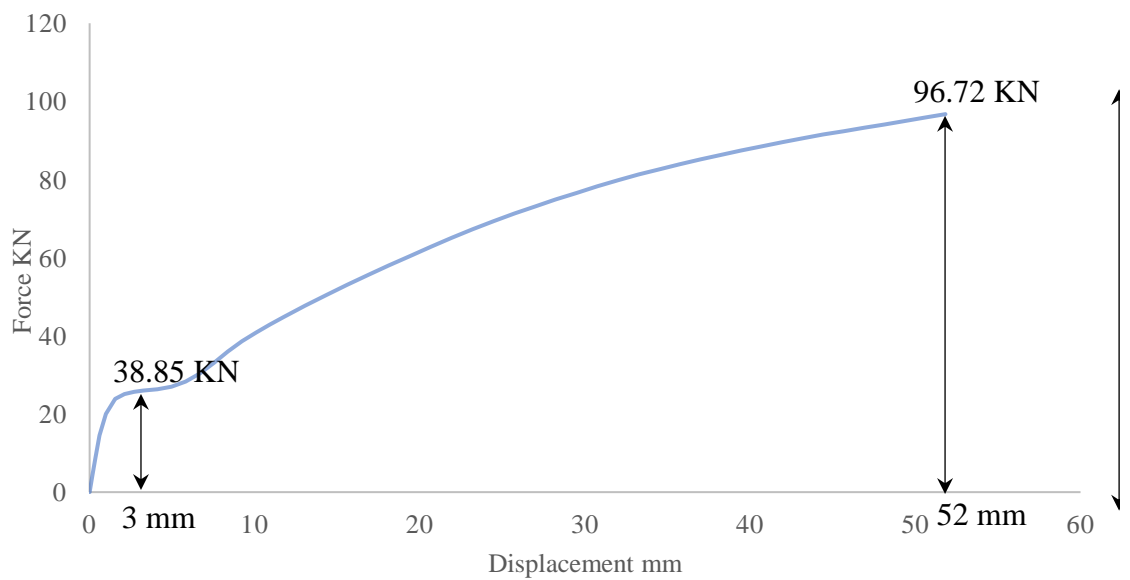


Figure 23 Force Vs Displacement from Numerical model with solid element

Shell model was created with same boundary and loading conditions as of solid element model. The models show a very close relation to the experiment when concerning the resistance at peak loading as shown in Fig.24.

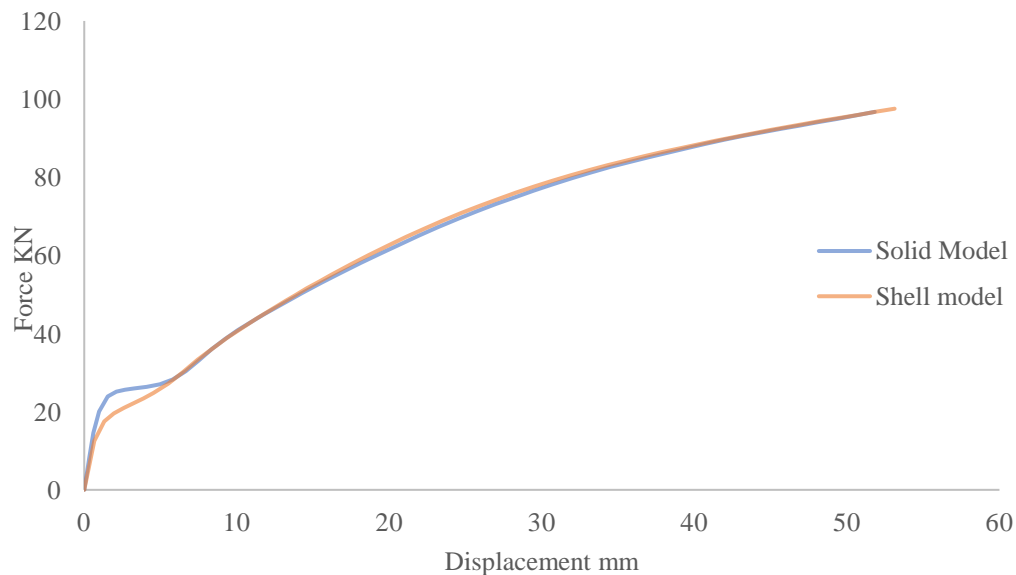


Figure 24 Force Vs Displacement comparison between solid and shell model

As mentioned in the previous chapter, only Welding residual stresses were applied on the Numerical model with solid elements as shown in Fig.25. According to EN 1999-1: 2007, for a MIG weld laid on unheated material and thickness $\leq 6\text{mm}$, the $b_{\text{haz}}=20\text{mm}$ is considered.

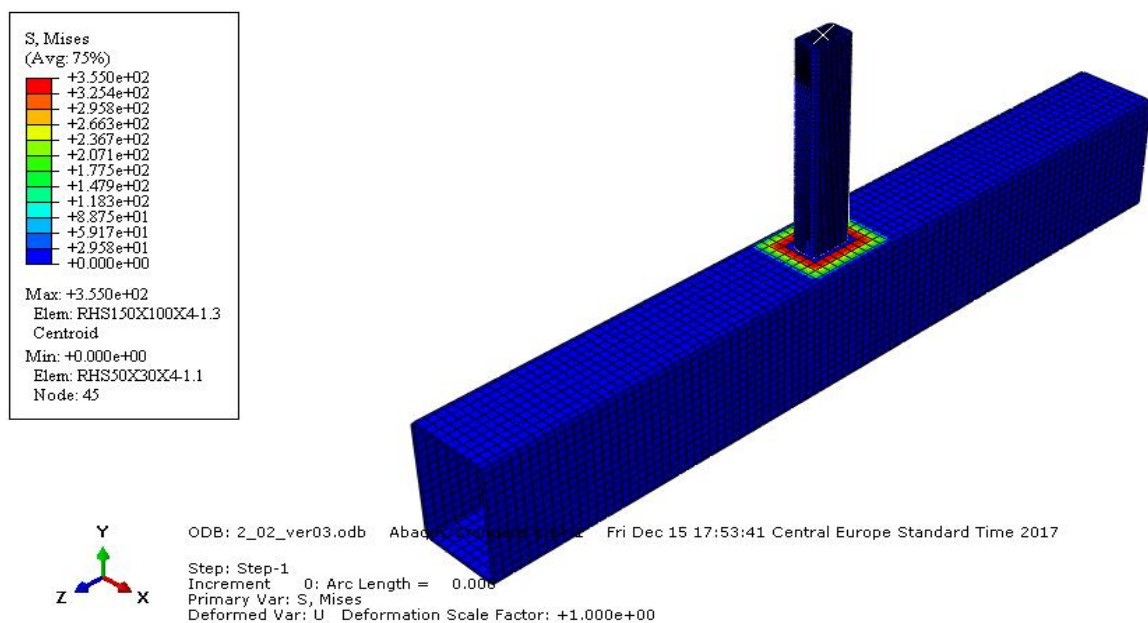


Figure 25 Application of Welding Residual Stresses on Solid Element Model

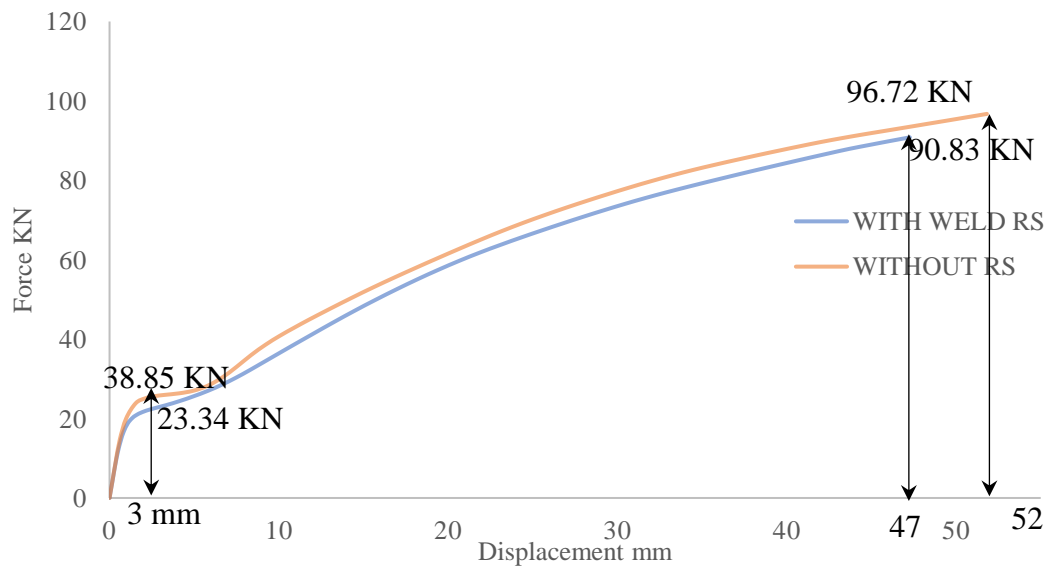


Figure 26 Force vs displacement comparison before and after applying weld RS

A 6% difference in the design resistance is observed after applying welding residual stresses and 13% difference in ultimate resistance is observed (Fig.26).

Shell model has been studied by applying residual stresses due to production first and then compared with the standard model without any residual stresses as shown in Fig.27.

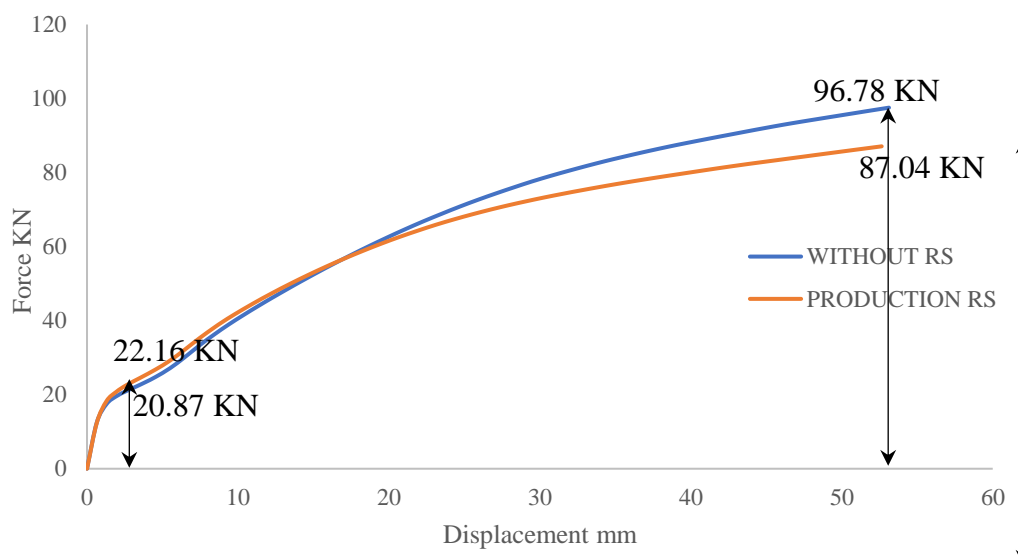


Figure 27 Force vs Displacement plot comparison before and after applying Production RS

Finally, Welding Residual stresses along with Production residual stresses are applied on the shell model as shown in Fig.28.

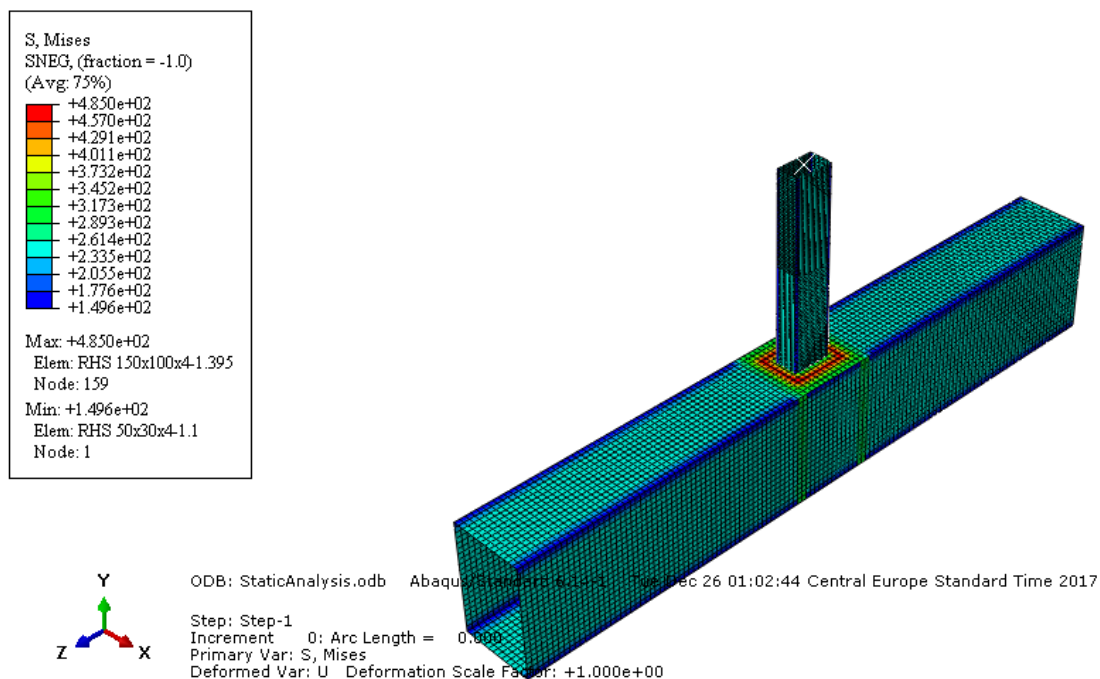


Figure 28 Applied Residual stresses due to Production and welding on the Shell element model

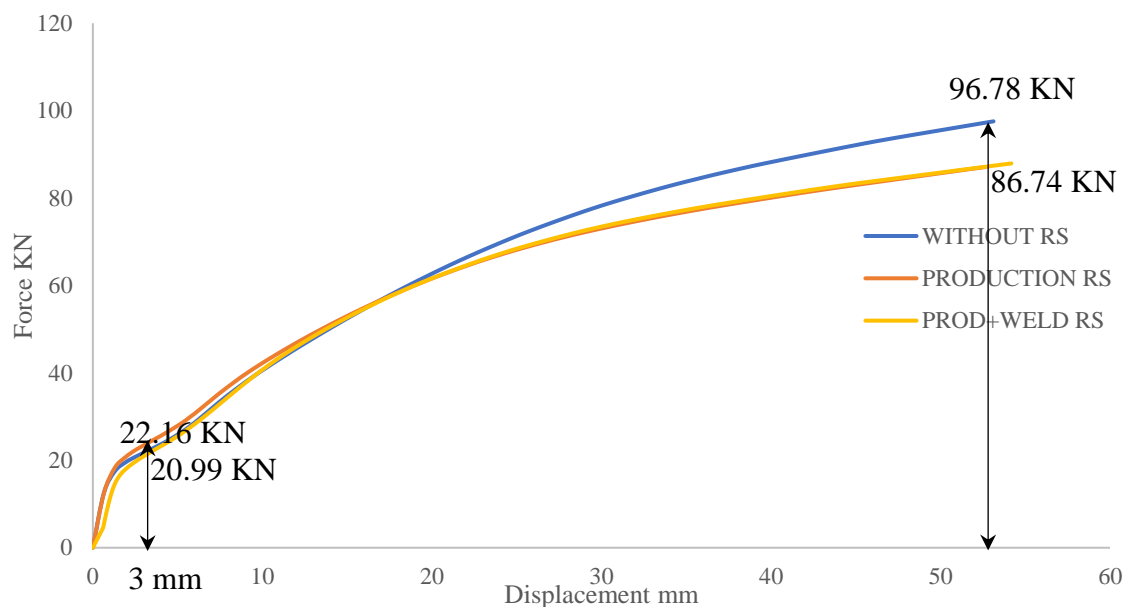


Figure 29 Force Vs Displacement Comparison between before and after application of RS
 A difference of 10% is seen in the Ultimate resistance after application of complete Residual Stresses(Fig.29).

6. Summary

6.1 Conclusions

Considering the obtained results on this dissertation, it can also be concluded that:

- Shell element FE model is not the most adequate numerical solution to verify the studied joint resistance but was studied to see the Production Residual stresses behavior when applied in layers.
- Shell element models provide us with the flexibility to apply residual stresses on each layer (Section points) where as Solid element model doesn't allow us to apply Residual stresses in layers (Can be applied in layers using SIGINI user routine but this method is quite complex and not easy for beginner level users).
- Resistance at 3% b_0 in case of solid element model after applying welding residual stresses was reduced by 40% which clearly implicates the effect of residual stresses in this zone.
- Influence of Residual stresses generated due to welding process at the joint reduces the Ultimate Resistance by 13% Approximately in the case of solid element numerical model.
- Production residual stresses were applied on the shell element model and only 6% reduction of resistance was seen at 3% b_0 whereas Ultimate resistance was decreased by 11%.
- Welding Residual stresses when applied along with the Production Residual stresses decrease resistance to 10% approximately at failure and 5% approximately at 3% b_0 . There is a very slight increase in resistance when applied together due to compressive Residual stress component which acts against the loading.

Finally, it can be concluded that influence of Residual Stresses on the resistance of hollow section joint is negligible at Ultimate resistance. So, it is not necessary to consider separately during the design of joint but where as in the range of elasticity they play some role depending on the component direction which needs to be considered.

6.2 Future Developments

Along the development of this dissertation, it was noted a necessity for more information in some fields of application where some further investigations could be taken, such as:

- Experiments should be done by also implementing measured values of imperfections on experiments, so that, in accordance to EN1993 1-6, these imperfections could be reflected on the FE models with accuracy.
- To perform convergence studies of shell element FE models by using different types of mesh elements and size to obtain accurate results
- To further analyse and improve the action of welded joint on FE models. It is necessary to refine the results by representing the true weld properties on the models.
- Although the model didn't show any major difference in Ultimate resistance, it is necessary to cross check the influence of these residual stresses by studying different types of model and Cross sections.
- To study further on the influence of residual stresses in the range of elasticity as the design standards allow the maximum deformation that can be considered only in this zone (3% of b_0)

References

- [1]. Jeffrey A. Packer, Jaap Wardenier, Xiao-Ling Zhao, Addie van der Vegte and Yoshiaki Kurobane, “Design guide for rectangular hollow section (RHS) joints under predominantly static loading”, Comité International pour le Développement et l'Etude de la Construction Tubulaire, 2009.
- [2]. CEN, European Committee for Standardization “EN 1993-1-1, Eurocode 3 – Design of steel structures – Part 1 -1: General rules and rules for buildings”, Brussels, 2005.
- [3]. CEN, European Committee for Standardization “EN 1993-1-8, Eurocode 3 – Design of steel structures – Part 1 -8: Design of joints”, Brussels, 2005.
- [4]. Hollow Section Joints by J.Wardenier, Delft University Press.
- [5]. Gurney T.R., Fatigue of Welded Structures, Cambridge Univ. Press, 1979.
- [6]. Krebs.J, Kassner.M, Alstom-LHB, “Influence of welding residual stresses on fatigue design of welded joints and components”, Welding in the World, 2007.
- [7]. Wardenier.J, “Hollow sections in structural applications”, Comité International pour le Développement et l'Etude de la Construction Tubulaire.
- [8]. Gardner.L, Bu.Y. and Theofanous.M, “Laser-welded stainless steel I-sections: Residual stress measurements and column buckling tests”, Engineering Structures, 2016.
- [9]. Paradowska.A, Price.J.W.H, Dayawansa.P, Kerezsi.B, Zhao.X-Land Ibrahim.R, “Measurement of residual stress Distribution in tubular joints considering post weld heat treatment”, Materials forum, 2006.
- [10]. Acevedo.C, Nussbaumer.A, “Residual Stress Estimation of Welded Tubular K-joints under Fatigue Loads”, Swiss Federal Institute of Technology, Lausanne, Switzerland.
- [11]. Handbook of Residual Stress and Deformation of Steel, ASM International society, 2002.
- [12]. De Matos R.M.M.P, Costa-Neves L.F, L.R.O. de Lima, Vellasco P.C.G.S, J.G.S. da Silva,” Resistance and elastic stiffness of RHS “T” joints: part I - axial brace loading”, Latin American Journal of Solids and Structures, 2015.
- [13]. X.-L. Zhao, “Deformation limit and ultimate strength of welded T-joints in cold-formed RHS sections”, Journal of Constructional Steel Research, 2000.
- [14]. Withers P. J. and Bhadeshia H. K. D. H, “Residual stress Part 1 – Measurement techniques”, Materials Science and Technology, 2001.

- [15]. Tso-Liang Teng, Ching Ping Fung, Peng Hsiang Chang, Wei Chun Yang, “Analysis of Residual stresses and distortions in T Joint Fillet Welds”, International Journal of Pressure Vessels and Pipings, 2001.
- [16]. Jandera.M and Machacek.J, “Residual stress influence on material properties and column behaviour of stainless steel SHS”, Thin-Walled Structures, Elsevier Journal, 2014.
- [17]. Peter W. Key and Gregory J. Hancock, “A theoretical investigation of the column behavior of cold formed Square Hollow Sections”, Thin-Walled Structures, Elsevier Journal, 1993.
- [18]IIW@(<http://www.iiwelding.org/TheIIW/Organization/Pages/WGStand.aspx>).(<http://www.iiwelding.org>). Visited on 26th November, 2017.
- [19]. Lu L, Winkel.H, Wardenier J, “Deformation limit for the ultimate strength of hollow sections joints”. Proceedings 6th International Symposium on Tubular Structures, Melbourne, Rotterdam, 1994.
- [20]. Simões da Silva.L, Santiago.A, “Manual de ligações metálicas”. Research project: Continuing Education in Structural Connections. CMM, Associação Portuguesa de Construção Metálica e Mista, Coimbra, Portugal, 2003.
- [21]. Dias da Silva.V, “Introdução á Análise Não Linear de Estruturas”. Faculdade de Ciências e Tecnologia da Universidade de Coimbra, Departamento de Engenharia Civil, Coimbra, Portugal, 2002.
- [22]. Xiangyang lu, “Influence of residual stress on fatigue failure of welded joints”, Doctoral Thesis, North Carolina State University.
- [23]. ABAQUS 6.13. Abaqus/CAE User’s Manual version 6.13, Dassault Systems Simulia Corp., Providence, RI, US, 2013.